INFORMATION TO USERS

This manuscript has been reproduced from the microfilm master. UMI films the text directly from the original or copy submitted. Thus, some thesis and dissertation copies are in typewriter face, while others may be from any type of computer printer.

The quality of this reproduction is dependent upon the quality of the copy submitted. Broken or indistinct print, colored or poor quality illustrations and photographs, print bleedthrough, substandard margins, and improper alignment can adversely affect reproduction.

In the unlikely event that the author did not send UMI a complete manuscript and there are missing pages, these will be noted. Also, if unauthorized copyright material had to be removed, a note will indicate the deletion.

Oversize materials (e.g., maps, drawings, charts) are reproduced by sectioning the original, beginning at the upper left-hand corner and continuing from left to right in equal sections with small overlaps.

Photographs included in the original manuscript have been reproduced xerographically in this copy. Higher quality 6" x 9" black and white photographic prints are available for any photographs or illustrations appearing in this copy for an additional charge. Contact UMI directly to order.

Bell & Howell Information and Learning
300 North Zeeb Road, Ann Arbor, MI 48106-1346 USA

UMI®
800-521-0600

Investigations of DNA Adducts of Adriamycin and Molecular Interactions Between DNA and xUBF Box 1

by

Ryan A. Luce

A dissertation submitted in partial fulfillment
of the requirements for the degree of

Doctor of Philosophy

University of Washington

1999

Program Authorized to Offer Degree: Chemistry

UMI Number: 9952864

Bell & Howell Information and Learning Company
300 North Zeeb Road
P.O. Box 1346
Ann Arbor, MI 48106-1346

Doctoral Dissertation

In presenting this dissertation in partial fulfillment of the requirements for the Doctoral degree at the University of Washington, I agree that the Library shall make its copies freely available for inspection. I further agree that extensive copying of the dissertation is allowable only for scholarly purposes, consistent with "fair use" as prescribed in the U.S. Copyright Law. Requests for copying or reproduction of this dissertation may be referred to Bell and Howell Information and Learning, 300 North Zeeb Road, P.O. Box 1346, Ann Arbor, MI 48106-1346, to whom the author has granted "the right to reproduce and sell (a) copies of the manuscript in microform and/or (b) printed copies of the manuscript made from microform."

Signature 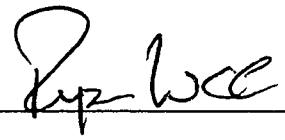

Date Dec. 13, 1999

University of Washington

Graduate School

This is to certify that I have examined this copy of a doctoral dissertation by

Ryan A. Luce

and have found that it is complete and satisfactory in all respects,
and that any and all revisions required by the final
examining committee have been made.

Chair of Supervisory Committee:

Paul B. Hopkins

Reading Committee:

Paul B. Hopkins

Bruce H. Robinson

Niels H. Andersen

Date: 12/10/99

University of Washington

Abstract

Investigations of DNA Adducts of Adriamycin and
Molecular Interactions Between DNA and xUBF Box 1

by Ryan A. Luce

Chairperson of the Supervisory Committee:
Professor Paul B. Hopkins

Department of Chemistry

Duplex DNA incubated with adriamycin, dithiothreitol (DTT) and Fe^{3+} under aerobic, aqueous conditions yields double stranded (DS) DNA bands by denaturing polyacrylamide gel electrophoresis (DPAGE) analysis, characteristic of DNAs which are interstrand cross-linked. Another laboratory provided evidence that formaldehyde produced under these conditions promotes the covalent linkage of adriamycin to one strand of DNA and suggested that this monoadduct results in this appearance of interstrand cross-linking upon DPAGE analysis. This dissertation provides strong support for this interpretation. We show that mixtures of DNA and adriamycin incubated with DTT/Fe^{3+}, H_2O_2, or formaldehyde all show DS DNA bands on DPAGE analysis. We have also developed an indirect, GC-MS analytical technique that quantitatively detects formation of this lesion. Using this technique, we show that the DS DNA bands and the formaldehyde-mediated lesion form with similar time courses, and in similar amounts. We also show that the DNA in the DS DNA bands contains approximately one such lesion per DNA, whereas the single stranded DNA is devoid of it. Finally, we cursorily examine the effect of sequence context on lesion formation. All of our results further support the interpretation that adriamycin does not create

interstrand cross-links in DNA, and that the DS DNA observed in DPAGE experiments derives from the formaldehyde-mediated monoadduct.

The N-terminal HMG box of xUBF (xUBF Box 1) is investigated for binding to synthetic oligonucleotides. A library of oligonucleotides with cisplatin intrastrand crosslinks was prepared and their relative affinities for xUBF Box 1 were determined using the electrophoretic mobility shift assay (EMSA). Due to the extremely poor binidng of these oligonucleotides, an electrophoretic binding assay based on the ability to compete with the binding of four-way junction DNA to xUBF Box 1 was developed. Although the efficacy of this competition assay is demonstrated, very little difference is seen in the affinity of the oligonucleotide library, either platinated or native, to xUBF Box 1. Despite this, an NMR-size sample of one of these platinated sequences has been prepared and its binding to the protein is currently being studied.

Table of Contents

List of Figures

List of Tables

List of Schemes

List of Abbreviations

4wj:	four-way junction DNA
A:	adenine
a.m.u.:	atomic mass units
C:	cytosine
CH_3CN:	acetonitrile
dA:	2'-deoxyadenosine
dC:	2'-deoxycytidine
dG:	2'-deoxyguanosine
dI:	2'-deoxyinosine
dT:	2'-deoxythymidine
DNA:	deoxyribonucleic acid
DPAGE:	denaturing polyacrylamide gel electrophoresis
DS:	double-stranded
DTT:	dithiothreitol
EDTA:	ethylenediamminetetraacetic acid
EMSA:	electrophoretic mobility shift assay
EPR:	electron paramagnetic resonance spectroscopy
ESMS:	electrospray mass spectrometry
G:	guanine
GC-MS:	gas chromatography – mass spectrometry
HEPES:	hydroxyethylpiperazineethanesulfonic acid
HMG:	high mobility group protein
HPLC:	high-pressure liquid chromatograhy
I:	inosine
ICL:	intrastrand crosslink
NMR:	nuclear magnetic resonance spectroscopy
Nu:	nucleophile
O.D.:	optical density units – the quantity of DNA, when dissolved in 1 mL water that will give an absorbance reading of 1 at 260 nm with a 1 cm pathlength
PAGE:	polyacrylamide gel electrophoresis
SS:	single-stranded
T:	thymidine
Tris:	trishydroxymethylaminomethane
UV:	ultra-violet
Vis:	visible
xUBF:	*xenopus laevis* upstream binding factor protein

Acknowledgements

I am grateful to a number of individuals who have helped during my graduate career. First and foremost, I would like to thank my advisor, Professor Paul B. Hopkins. I would hope to emulate his high standards, professionalism, and enthusiasm for science in my own career. I would also like to thank my Hopkins group comrade, Eric Harwood, for going through this entire endeavor with me. Dr. Snorri Th. Sigurdsson has been extremely helpful in development of research projects. Former Hopkins group members Huifang Huang, Steve Alley, Manuel Paz, and Paula Fischhaber have all been excellent teachers of science as well. I would also like to thank Tamara Okonogi, Angie Kantola, Dr. Rachel Klevit, and Dr. Bruce Robinson for their various collaborations.

Finally, I would like to thank the myriad friends and family in my life who are ultimately responsible for any success I might have. Friends include Adam Schafer, Tobin Thompson, and Jon Grabowski. Current and future family includes my sister Megan, my parents Ned and B.J., and my fiancé Tina Schwien. To them, I owe a debt of gratitude I can never repay.

Chapter I. Introduction: Cancer, DNA and Adriamycin

Significance and treatment of cancer

With the possible exception of HIV, no diagnosis inspires more fear than cancer. Cancer can come in a number of different forms, making it very difficult to find a cure.(*1, 2*) Essentially, cancer is the unregulated and unchecked growth of cells. As these cells multiply, they often revert to an undifferentiated state.(*1, 3, 4*) These cells multiply uncontrollably, metastasize into other areas of the body, and eventually cause death if untreated.

There are over a million new cases of cancer each year in the United States.(*2*) That number fails to include more than 500,000 cases of skin cancer each year. Five hundred forty thousand people died in 1994 due to cancer, making the disease the cause of approximately one-fifth of all deaths in the United States.(*5*) Due to the tremendous personal toll this disease exacts, finding better treatments for cancer is, as it should be, a major focus for medical research.

Compared to surgery and radiation, chemotherapy is a relatively new way of treating cancer. Chemotherapy is simply defined as the treatment of disease with chemicals. Radiation and surgery had both been used for decades before the successful use of chemotherapy.(*1*) The first commonly used chemotherapeutic agent was a nitrogen mustard, mechlorethamine. The usefulness of this compound was discovered during World War II.(*2*) Since this time, several different chemotherapeutic agents have been developed with various potencies and cancer targets. The development of these antitumor agents, along with improvements in the surgical and radiotherapy strategies, has dramatically changed the outlook of cancer patients. The 5-year survival rate of cancer patients has increased dramatically in the last 60 years – 1930: 20%; 1940: 25%; 1960: 33%; and 1994: 53%.(*5*)

A large number of chemotherapeutic agents are currently used for cancer treatment.. Most of these antitumor agents are thought to garner their activity through interactions with DNA.(*6-10*) In order to understand how these antitumor agents work, one must understand the structure and chemistry of DNA.

The importance of deoxyribonucleic acid (DNA)

The structure of DNA was determined by Watson and Crick in 1953.(*11*) Since this time, it has quickly become clear that DNA is involved in all aspects of cell regulation. This includes cell differentiation, apoptosis, and growth.(*4*) In fact, DNA is almost always ultimately involved in the generation of cancer.(*1, 12, 13*)

DNA plays several roles in the advent of cancer, the most common of which is chromosomal damage. This can occur either through chemical carcinogens, ultraviolet (UV) light, or radiation. Some viruses have also been shown to be involved in cancer.(*1*) Thirdly, some individuals and families have a predisposition for cancer that is inherited genetically. Finally, telomerase activity is often seen in cancer cells.(*14*) Telomerase is an enzyme that is used to rebuild the end caps of chromosomes, called telomeres, after DNA replication. In each of these four scenarios, DNA is ultimately responsible for the appearance of cancer. As a result, DNA is a good target for manipulation when attempting to fight cancer.

With few exceptions, the majority of antitumor agents act by either inhibiting the synthesis of DNA or by interfering with its proper operation.(*2*) One of the most commonly used and potent antitumor agents is adriamycin (**1**).(*2, 15*) This drug, also called doxorubicin, is thought to derive its activity from interactions with DNA.(*6-10*)

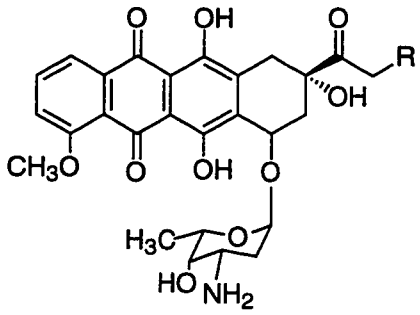

(**1**) adriamycin or doxorubicin, R = OH

(**2**) daunomycin or daunorubicin, R = H

Adriamycin

Daunomycin (**2**), the precursor to adriamycin, was discovered independently by two different research groups in 1963. In the laboratories of Rhone-Poulenc in Paris, it was isolated from *Streptomyces caeruleorubidas* and given the name rubidomycin due to its ruby color.(*16, 17*) At Farmitalia in Italy, it was isolated from *Streptomyces peucetius*, a bacterial strain from a soil sample collected on the grounds of the Castel del Monte, a 12th century castle in southeastern Italy.(*18, 19*) Farmitalia named their compound daunomycin because a pre-Roman tribe called Daunii once lived in the region where the soil sample was found.(*20*) Once these two groups made their research public, it was promptly noticed that they had discovered the same compound. In order to give credit to both groups, the name daunorubicin was embraced as the international nonproprietary name.(*20*) The terms daunomycin and daunorubicin are both used today. It quickly became apparent that this new anthracycline antibiotic had a potent ability to fight tumor growth.(*21, 22*) After the structure of daunomycin was determined,(*23, 24*) there was considerable interest within the scientific community in developing structurally similar compounds and determining their antitumor activity.

Federico Arcamone exposed *Stretptomyces peucetius* to the mutagen N-nitroso-N-methyl urethane, hoping to develop new strains of the bacteria that would yield

structurally similar analogs of daunorubicin. Eventually, his research group was able to isolate adriamycin from a strain of the bacteria called *Streptomyces peucetius var. caesius*[Arcamone, 1969 #1 its name having originated from the blue-green color of its mycelium. Arcamone named the compound adriamycin because of the Adriatic Sea's proximity to Castel del Monte, the city where the original bacterial strain was found. Adriamycin is now a registered trade name and the non-proprietary name is doxorubicin.(*20*) The terms doxorubicin and adriamycin are both used today. The structure of adriamycin is essentially identical to that of daunomycin, with the exception of the additional hydroxyl group at C-14. Almost immediately, it was shown that adriamycin was also a potent antitumor agent, potentially stronger than daunomycin.(*25*) Adriamycin has now been used as an antitumor agent for more than 20 years.(*20, 26, 27*)

Adriamycin is one of the most widely used antitumor compounds. It is currently used in several types of cancer, including leukemia, Hodgkin's and non-Hodgkin's lymphomas, and carcinomas of the breast, lung, and ovary.(*28, 29*) It also has the advantage of not being antagonistic with any other commonly used chemotherapeutic agents. Additionally, it can be administered with very similar efficacy using a variety of different schedules, either monthly, weekly, or through prolonged infusion. These characteristics have made adriamycin a standard drug to use in combination drug chemotherapy for a variety of cancers.(*29*)

Use of adriamycin, however, is not entirely devoid of problems. There are two main concerns associated with the treatment of tumors by adriamycin. First, cancer cells can develop resistance to adriamycin. The most common mechanism *in vitro* for the development of resistance is increased transport of drug out of cells through amplification of the gene for P-170 glycoprotein. Cells which have been exposed to adriamycin for a prolonged period and have demonstrated resistance have higher levels

of this protein.(*2*) The second concern, which is of potentially higher importance, is the cardiotoxicity of adriamycin. Adriamycin has long been associated with delayed cardiomyopathy. This toxicity of the heart is cumulative with continued use of the drug.(*30-32*) This side effect of adriamycin is the main reason for limiting the dose that can be used in cancer patients.(*31*) The limit on tne amount of adriamycin that can be prescribed is approximately 450-500 mg/m^2 - which is associated with a 1%-10% chance of clinically evident cardiotoxicity.(*29*) Treatment protocols have been developed where by the cardiotoxicity of adriamycin is decreased by concurrent use of antioxidants.(*32*) These protocols, however, have not been completely successful.

In efforts to circumvent these obstacles, over 2000 analogs of adriamycin have been developed. Unfortunately, none of these analogs are more effective than adriamycin.(*20*) The problem is that the precise nature of how adriamycin works is unknown.(*33*) In order to be able to develop better analogs of adriamycin (or devise more effective treatment regimens), a better understanding of how adriamycin works is needed.

Potential modes of action for adriamycin

It is possible that the largest barrier to a thorough understanding of how adriamycin works is its large number of possible modes of action. It is also very probable that adriamycin works through more than one of several pathways, further complicating the picture.(*33*) Thankfully, critical to each of these pathways is the binding of adriamycin to DNA. Adriamycin binds to DNA very tightly, with a binding constant of approximately $3 \times 10^7\ M^{-1}$ and a $\Delta G°$ of -9.9 kcal mol^{-1}.(*34*) When living cells are treated with adriamycin, more than 99.8% of the drug is found bound to DNA.(*7*) The first and simplest of these potential mechanisms is the suggestion that

adriamycin simply inhibits DNA biosynthesis.(*33*) Most researchers, however, are of the opinion that the mechanism is more convoluted than that.

One reason why the drug's mechanism is thought to be more complex is that adriamycin and daunomycin are quinones. There are a number of enzymes that can act as electron donors to these structures. These include cytochrome P450 reductase, NADH dehydrogenase, and xanthine oxidase – all enzymes that catalyze reduction and/or oxidation reactions.(*33*) Adriamycin can be sequentially reduced by a single electron, yielding a semiquinone (**3**) and a hydroquinone (**4, Scheme 1**). The resulting semiquinone free radicals may induce free-radical injury to DNA either through direct interaction or after interactions with molecular oxygen to form superoxides, hydroxyl radicals, and peroxides.(*33*) The ability to be reduced and then subsequently oxidized by oxygen is known as redox cycling. Redox cycling and the concurrent formation of reactive oxygen species are also thought to be the cause of the cardiotoxicity of adriamycin.(*35*)

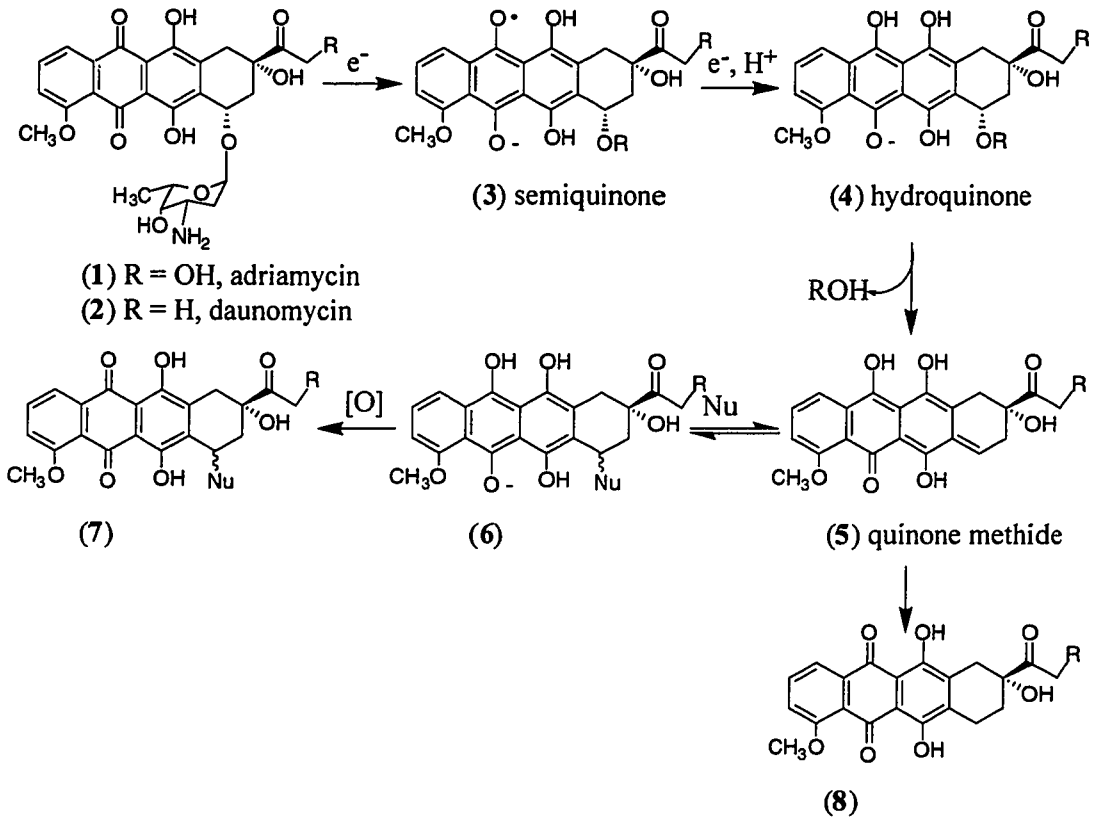

Scheme 1. One electron reductions of adriamycin and daunomycin.(*35*)

Another potential mechanism for the activity of adriamycin is its ability to inhibit the activity of two classes of enzymes associated with controlling the topology of DNA. The first of these is the helicases. The role of helicases is to separate duplex DNA into single strands so that replication or transcription can occur. It has been shown that binding of adriamycin to DNA inhibits the action of these enzymes.(*33, 36-39*) The second class is the topoisomerases. Topoisomerases are able to cleave either one or both strands of the DNA duplex in order for one strand to rotate freely around the other. This allows for either the winding or unwinding of DNA. Topoisomerase II and adriamycin form a ternary drug-DNA-enzyme complex which traps DNA strand passage intermediates, leading to single and double strand breaks in DNA.(*40-43*) Although inhibition of topoisomerase II is generally thought to be the most probable

source of adriamycin's activity, one could argue that helicase is a more likely target because its activity is dependent on its ability to processively slide along the DNA helix.(*36*) Topoisomerase II, on the other hand, aims for a single target, making it easier to miss the DNA-bound adriamycin. The structure of the ternary complex of adriamycin, DNA, and topoisomerase II is unknown. Wang and co-workers, however, have reported the single-crystal x-ray structure of both the non-covalent intercalation complex of adriamycin and daunomycin with DNA(*44, 45*) as well as a formaldehyde-mediated covalently linked complex.(*46, 47*)

Crosslinking of DNA with adriamycin

Given the lack of concrete knowledge as to exactly how adriamycin works, a number of researchers have been investigating this antitumor agent. Prior to the beginning of the research outlined in this dissertation, Phillips and co-workers investigated the reactions of adriamycin with duplex DNA in the presence of reducing agents.(*48, 49*) (A number of DNA alkylating agents are activated by reductive conditions.) Initially, Phillips and coworkers observed transcriptional blockages at guanine residues of 5'-GC sequences in DNA that had previously been incubated with adriamycin, dithiothreitol (DTT), and Fe^{3+}.(*50*) Subsequent experiments showed that DNA which was treated with reductively activated adriamycin displayed electrophoretic mobility similar to that of double-stranded (DS) DNA when subjected to denaturing polyacrylamide gel electrophoresis (DPAGE). This is a characteristic of the presence of interstrand DNA cross-links (**Figure 1**).(*48*)

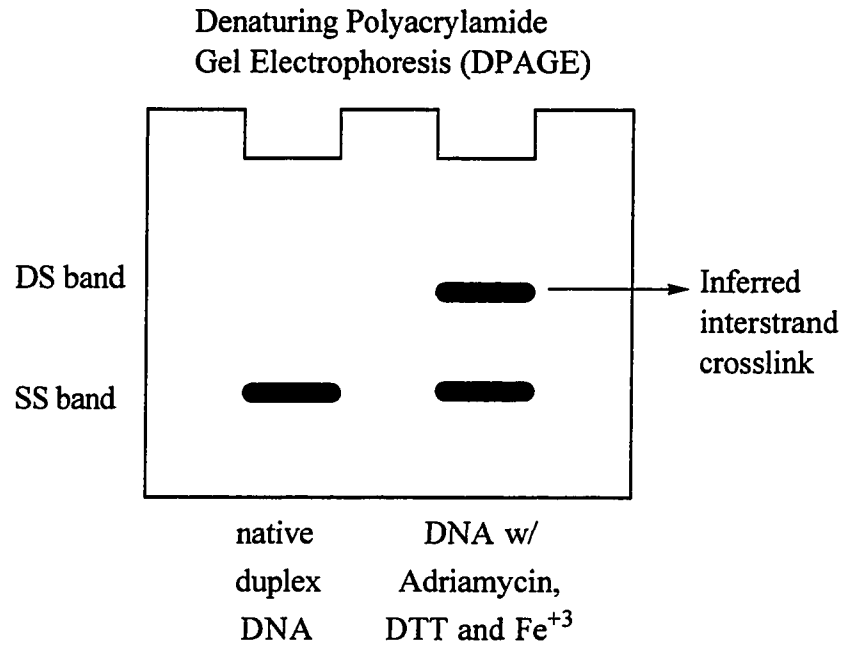

Figure 1. Schematic of DPAGE.

Deoxyinosine replacement experiments revealed that N2 of deoxyguanosine played a primary role in the formation of this denaturation-resistant DS DNA.(*48, 49*) For example, an 8-fold reduction in the amount of the DS DNA band was seen when one deoxyguanosine in the $[5'\text{-d(GC)}]_2$ duplex was replaced by deoxyinosine.(*49*) Phillips and co-workers concluded that the major component of the DS DNA was the result of an interstrand cross-link between the N2 atoms of the two guanines. They suggested that the intermediate in formation of these cross-links was the quinone methide (**5**) which was formed by adriamycin in the presence of DTT.(*48, 51*) The quinone methide provided an electrophile for N2 of dG on one strand. Previously, it had been shown that menogaril (**10**), a compound similar to adriamycin, alkylated N2 of 2'-deoxyguanosine when reductively activated under anaerobic conditions by the one-electron-reducing agent bi(3,5-dimethyl-5-(hydoxymethyl)-2-oxomorpholin-3-yl) (DHM-3 dimer) (**Scheme 2**).(*52*) Phillips and co-workers were unable, however, to suggest where the other strand of DNA might attach to adriamycin.

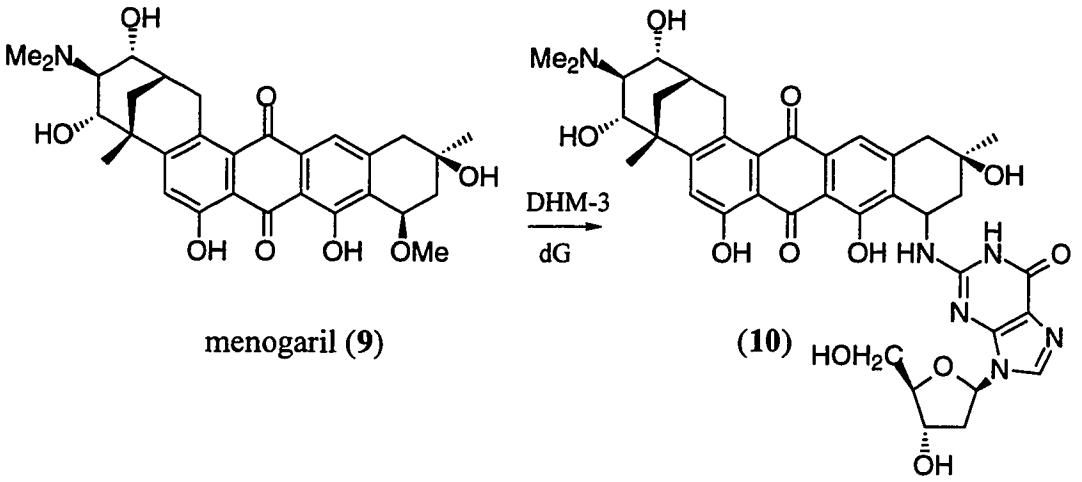

menogaril (**9**) (**10**)

Scheme 2. Reductive activation of menogaril in the presence of dG.

Formaldehyde-mediated alkylation of DNA by adriamycin

Because alkylation of DNA is a characteristic of several antitumor agents and toxins, we attempted to characterize these interstrand cross-links that had been observed by Phillips. While this research was in progress, Koch and co-workers related in an insightful study (*53, 54*) the observations of Phillips and co-workers to the formaldehyde-mediated covalent complex of adriamycin and DNA provided by Wang and co-workers.(*46, 47*) Koch's laboratory determined that reactions of DNA duplex $[5'\text{-d(GCGCGCGC)}]_2$ with adriamycin, activated by either DTT/Fe^{3+}, H_2O_2, or CH_2O, all gave the same adriamycin-DNA complex. Mass spectrometric analysis revealed this complex to have a molecular mass corresponding to the combined mass of single stranded DNA, adriamycin, and a methylene unit, minus the mass of two hydrogen atoms. This mass is consistent with the formaldehyde-mediated lesion that Wang and co-workers had studied by x-ray crystallography. Koch and co-workers suggested that the formaldehyde results from H_2O_2-promoted oxidation of Tris buffer or Baeyer-Villiger oxidation of adriamycin itself. The H_2O_2 is generated by reduction of O_2 in the DTT/Fe^{3+} mixture.(*53, 54*) They have also investigated other redox reaction systems

and demonstrated that they form the same adriamycin-DNA complex as the previously mentioned activating agents.(*55*)

In the structure that Wang and co-workers determined for the formaldehyde-mediated coupling of adriamycin to DNA, adriamycin is linked through its amino group to N2 of a deoxyguanosine residue through a methylene group (**11**, **Figure 2**).(*46, 47*) Adriamycin is essentially composed of two units: the amino sugar and the anthraquinone ring (or aglycon). Adriamycin intercalates DNA, with the anthraquinone ring placed in between two successive base pairs, and the amino sugar lays down in the minor groove (**Figure 3**). In the presence of formaldehyde and with the appropriate DNA sequence, a methylene bridge is formed between the amino group of adriamycin and the exocyclic amino group of deoxyguanosine of DNA. With the exception of the addition of a methylene group, the structures of adriamycin and daunomycin bound both in non-covalent and covalent fashion are virtually identical. The methylene group in this aminal presumably has its origin in formaldehyde. This is consistent with the studies by Chaires and co-workers who determined that N2 of deoxyguanosine in DNA, the amino group of adriamycin, and formaldehyde are necessary and sufficient for lesion formation.(*56*)

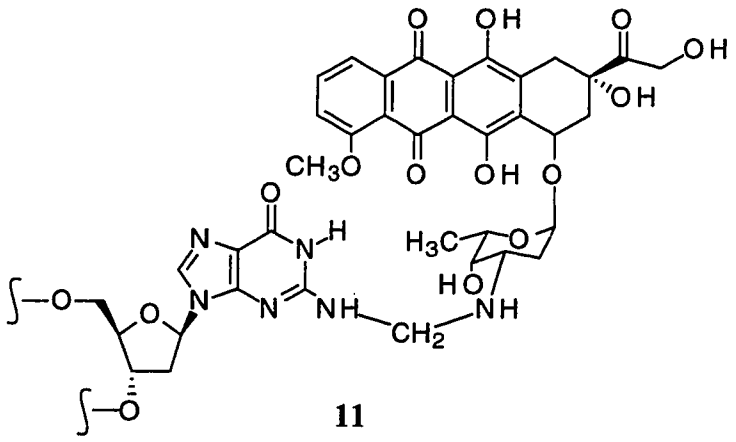

11

Figure 2. Adriamycin linked to dG of DNA via formaldehyde.

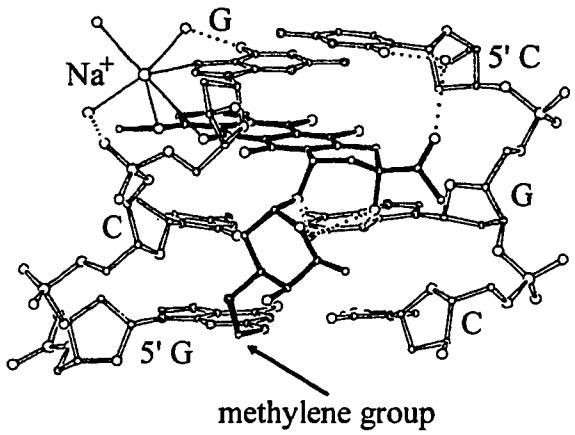

Figure 3. X-ray crystal structure of adriamycin covalently attached to DNA via formaldehyde. Figure taken from reference.(*46*)

Koch and co-workers have proposed that the DS DNA bands reported by Phillips are not due to interstrand cross-links, but rather have their origin in resistance to denaturation caused by **11**. This is consistent with the increased melting point of DNA upon incorporation of **11** compared to adriamycin non-covalently bound to DNA.(*56*) Koch and co-workers further suggest that important hydrogen bonding interactions between adriamycin's 9-OH and N2 of dG on the non-alkylated strand (**Figure 3**) create a "virtual cross-link." This explains the 5'-GC sequence selectivity of the DS DNA formation as well as the lability of the lesion observed by Phillips and co-workers.

After completion of the adriamycin research in our lab, Zeman, Phillips, and Crothers published a study characterizing the formladehyde-mediated complex by NMR.(*57*) It was concluded in both cases that the major product was **11**. They also determined that incorporation of lesion **11** greatly decreased the rate of strand exchange for duplex DNA in the presence of excess single stranded DNA which has a complementary sequence.(*57*) There was, however, no experimental data which

conclusively showed that lesion **11** is responsible for the DS DNA observed by DPAGE.

In spite of strong circumstantial evidence supporting the explanation by Koch and co-workers concerning the structural origin of the DS bands, potential contradictions remained unresolved. Chaires demonstrated that the formaldehyde-mediated coupling of daunorubicin to DNA occurs at guanine in *any* sequence. Despite this, Phillips' experiments (which we have since confirmed) have shown that only DNA containing the sequence [5'-d$(GC)_2$] affords the DS bands by DPAGE. Given these circumstances, it seemed reasonable to seek further evidence that the formaldehyde-mediated covalent linkage is the origin of the DS DNA bands. This evidence is provided within this thesis. In the course of this study, a quantitative and sequence independent assay for lesion **11** using gas chromatography - mass spectrometry (GC-MS) was developed. We have used this assay to provide further structural evidence for **11** as the causative lesion of DS bands in DPAGE. We have conclusively shown that lesion **11** is necessary, but not sufficient, for the formation of DS DNA seen by DPAGE analysis of DNA which has been incubated with adriamycin, activated by either DTT/Fe^{3+}, H_2O_2, or CH_2O. These results further support the interpretation of Koch et al. that adriamycin does not create interstrand cross-links in DNA, and that the DS DNA observed in DPAGE experiments derives from the covalent monoadduct **11**. Moreover, we have developed a quantitative and versatile assay for detection of lesion **11** in a variety of systems, potentially even *in vivo*.

Binding of an HMG protein to DNA

Chapters II and III of this dissertation detail the investigations into DNA's interactions with adriamycin. This dissertation will also, however, outline the preliminary results of investigations into the interactions of chemically altered

oligonucleotides (primarily cisplatin intrastrand crosslinks) with high mobility group (HMG) proteins. These results, as well as accompanying material, are covered in Chapter IV and Chapter V.

Chapter II. Initial DPAGE with adriamycin and development of GC-MS assay.

DPAGE analysis of DNA admixed with adriamycin and activated by DTT/Fe^{3+}, H_2O_2, or CH_2O

The first goal was to demonstrate that formation of lesion **11** causes the double-stranded (DS) bands seen by Phillips and co-workers with reductively activated adriamycin. If lesion **11** is the source of the DS DNA observed by Phillips and co-workers,(*48, 49*) and if activation by either DTT/Fe^{3+}, H_2O_2, or CH_2O leads to the production of lesion **11** as reported by Koch and co-workers,(*53, 54*) then activation by any one of the above three agents should result in observation of these DS DNA bands by DPAGE. Similar to the experiments performed by Phillips and co-workers, 5'-radiolabeled DNA duplex I (100 μM) was incubated (40 mM Tris base, pH 8.0, 50 mM KCl, 3 mM $MgCl_2$, 0.1 mM EDTA) in the dark at 37°C with or without adriamycin (200 μM) and various other reagents (**Figure 4**). After ethanol precipitation and drying, samples were dissolved in 5 M aqueous urea loading buffer and analyzed by 20% DPAGE. The DS DNA (approximately one-half the mobility of single strands, **Figure 4**) was quantified by phosphorimagery. DS DNA was seen for each of the three activating agents in the indicated yield: DTT/Fe^{3+} - 19%; H_2O_2 - 6%, CH_2O - 73%, but only when adriamycin was present. Incubation of the DNA with adriamycin alone yielded only single stranded bands. This demonstrated that activation of adriamycin by either H_2O_2 or CH_2O afforded the DS DNA bands, similar to the observations of Phillips and co-workers with

DNA Duplex I: 5' TTG AAG CAA CGA AGT T
3' AAC TTC GTT GCT TCA A

Sequence of DNA Duplex **I.**

DTT/Fe^{3+} activation.(*48, 49*) This is consistent with the suggestion that lesion **11** is responsible for the DS DNA.

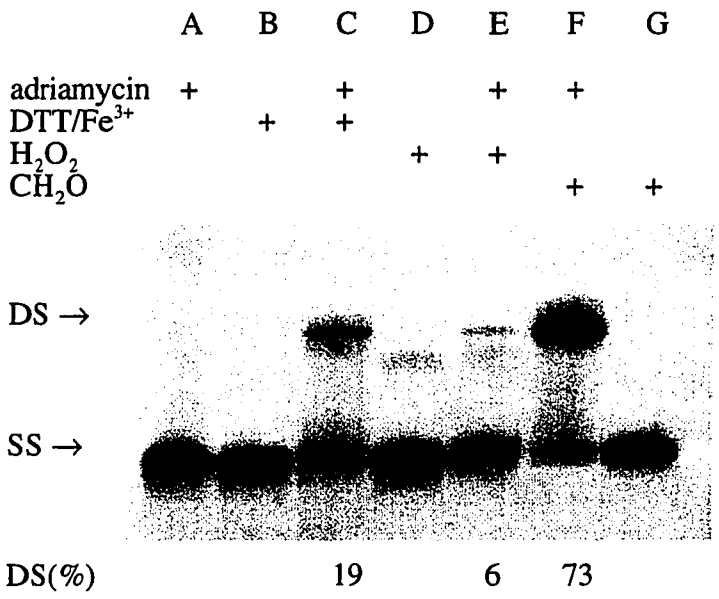

Figure 4. DPAGE analysis of DNA duplex I and adriamycin. All reactions were performed in the dark at 37°C using 100 μM DNA duplex I in Tris buffer. (A) 200 μM adriamycin; (B) 7 mM DTT, 40 μM $Fe(Cl)_3$; (C) 7 mM DTT, 40 μM $Fe(Cl)_3$, 200 μM adriamycin; (D) 5 mM H_2O_2, 200 μM adriamycin; (F) 1 mM CH_2O, 200 μM adriamycin; (G) 1 mM CH_2O. All reactions were allowed to progress 96 hours except F and G, which was stopped after 24 hours.

*Failings of DPAGE analysis of lesion **11***

The problem with DPAGE, however, is that it is not a consistent detection method for lesion **11**. Adriamycin is covalently attached to only one of the two strands of the DNA duplex. Non-covalent interactions between adriamycin and the non-alkylated strand, as well as non-covalent interactions between the two DNA strands themselves, are essential for keeping the duplex together under the denaturing conditions of DPAGE. This makes the results of the DPAGE experiment difficult to predict for various oligonucleotides depending on their G-C base pair content and length. If the

length of the DNA was too short or if there were not enough G-C base pairs, no DS band would be seen even if it contained the 5'-GC sequence (data not shown). Another problem is that small variations in experimental conditions lead to drastically different results. The temperature, time length, percentage of urea, and composition of loading buffer all affected the outcome of the DPAGE experiments when detecting lesion **11**. One could imagine that these different variables might somehow be combined and computed to determine how "denaturing" a particular DPAGE experiment was. An experiment must be "denaturing" enough to pull apart the two strands of a DNA duplex when adriamycin is simply non-covalently bound. It can't be so "denaturing", however, that lesion **11** is not strong enough to hold the duplex together. This level of "denaturing" would obviously be different for various oligonucleotide sequences. Given this level of complexity, we decided to attempt to develop another assay for detection of lesion **11** that would be quantitative and flexible for a variety of oligonucleotides.

Detection of lesion 11

The simplest way to prove that lesion **11** is present would be to isolate the formaldehyde-mediated conjugate of adriamycin with deoxyguanosine. Many DNA alkylating agents that are conjugated to a specific DNA base have been isolated by enzymatic digestion. Attempts, however, to isolate the conjugate of adriamycin with deoxyguanosine implicit in **11** following enzymatic digestion of the DNA phosphodiester backbone returned only unmodified nucleosides and adriamycin. It is presumed that free of duplex DNA, the aminal in **11** is too vulnerable to hydrolysis. This is consistent with the reversibility of lesion formation.(*49, 53, 58*)

Non-symmetrical aminals are much less prevalent than symmetrical aminals in the world of synthetic organic chemistry.(*59*) As a result, not much has been reported about the mechanism of their decomposition. Despite this, there has been at least one

study of a non-symmetrical aminal that involved an aliphatic and aromatic amine. The authors of that study suggested, but did not prove, that the iminium ion remained with the aliphatic amine and that the aromatic amine was the initial leaving group.(*60*) With regard to compound **11**, we believed that the electron-withdrawing dG would be the initial leaving group and that the iminium ion intermediate would be complexed with adriamycin (**Scheme 3**).

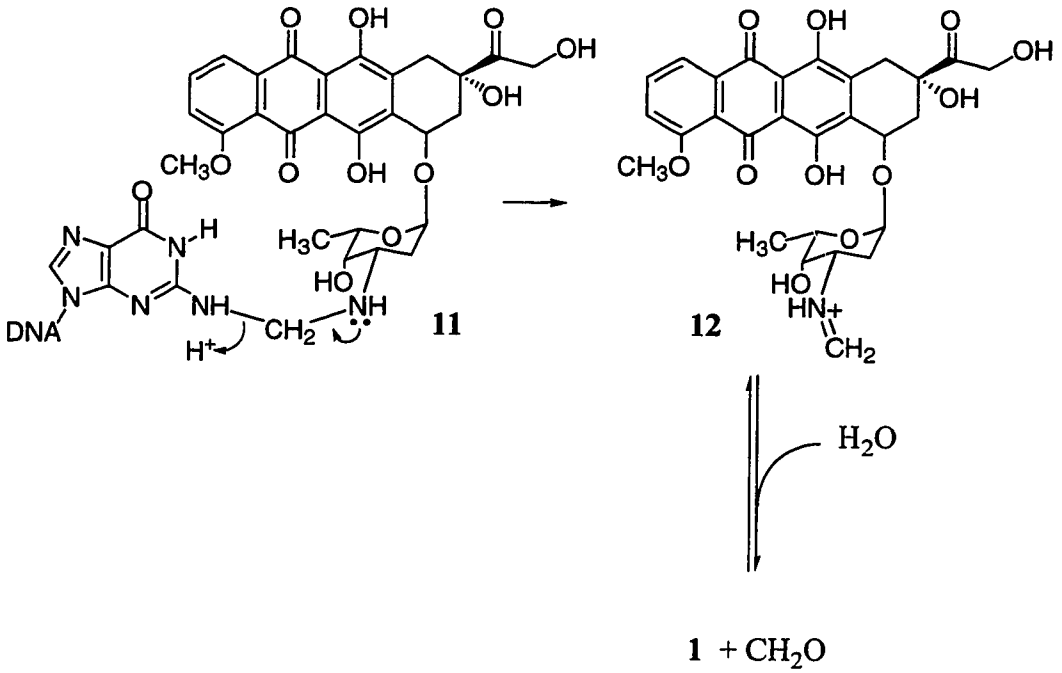

Scheme 3. Hydrolysis of aminal 11. It was initially assumed that **11** would hydrolyze leaving the iminium ion with adriamycin.

Given our assumption that the iminium ion would be on the adriamycin moiety of the aminal, we set out to capture it by reduction. Previously, formaldehyde was used to crosslink two deoxyadenosine bases.(*61*) In the case of that aminal, the decomposition intermediate was captured by a reducing agent, yielding (N6-methyl)-deoxyadenosine. We elected therefore to detect **11** indirectly, by trapping the iminium ion intermediate **12** in the hydrolysis (**Scheme 3**). In order to generate an authentic

sample of the methylated daunosamine sugar, adriamycin was reacted with a large excess of CH_2O in 2:1 CH_3CN:H_2O in the presence of 67 μM $NaCNBH_3$.(*62*) HPLC affords an approximately 1:1:1 ratio of three broad peaks, the first of which was determined to be adriamycin through comparison of retention times and co-injection (**Figure 5**). The second and third peaks were determined by ESMS to be N-methyl adriamycin (**1b**) (MH^+ = 558.5) and N,N-dimethyl adriamycin (**1c**) (MH^+ = 572.5), respectively. Subsequent GC-MS analysis of adriamycin and **1b** after borohydride reduction and acetylation showed three major ions for each (**5a**: m/e 56, 98, 158; **5b**: m/e 70, 112, 172) (**Figure 8**). This is consistent with methylation having occurred at the amino group.

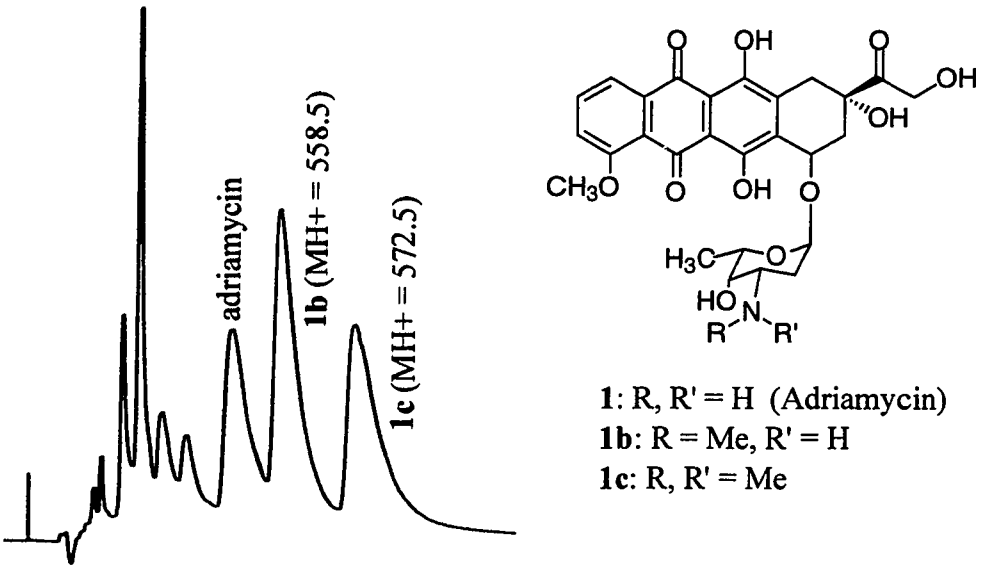

Figure 5. HPLC analysis of reductive methylation of adriamycin. The peak for adriamycin was determined by electrospray mass spectrometry (ES-MS) and co-injection with an authentic sample. The structures of **1b** and **1c** were confirmed by ES-MS as well as gas chromatography – mass spectrometry (GC-MS) analysis of their respective reduced and acetylated amino sugars.

It was clear that the iminium ion intermediate **12** could be captured by reductive methylation of adriamycin in the presence of $NaCNBH_3$. At this point, DNA treated

with formaldehyde and adriamycin was exposed to the same reductive conditions used to generate N-methyl adriamycin. Despite this, after enzymatic digestion, HPLC analysis again returned only unmodified nucleosides and adriamycin. Neither N-methyl adriamycin (**1b**) nor (N2-methyl)-deoxyguanosine were observed. In retrospect, we should have expected this. In the previously mentioned isolation of (N6-methyl)-deoxyadenosine from the formaldehyde-mediated coupling of two dA bases, saturated borohydride conditions returned only a 40% yield of expected methylation.(*61*) Given that we were using a much weaker reducing agent (cyanoborohydride vs. borohydride) and at orders of magnitude lower in concentration (<100 μM vs. ~5 M), it is not surprising that aminal **11** did not yield a methylated derivative.

Because of the instability of **11**, we elected to use saturated borohydride conditions to capture the iminium ion intermediate **12**. Unfortunately, these reducing conditions force elimination and reduction of the daunosamine sugar. Ironically, this is the same elimination that was theorized to be important to the crosslinking initially considered by Phillips.(*48, 51*) Loss of the chromophore prohibits detection of the normethyl and N-methyl dihydro daunosamine derivatives by HPLC methods. As a result, a new method of detecting these derivatives needed to be developed.

Coupling amino sugars to fluorescein isothioscyanate

In order to still use HPLC as a detection method for the methylated adriamycin derivative, we investigated the possibility of using fluorescein isothiocyanate as a marker. After exposure to 5M $NaBH_4$, model amino sugars glucosamine and N-methyl glucamine were successfully coupled to fluorescein isothiocyanate (**Scheme 4**). Problems arose, however, with the isothiocyanate coupling of the reduced amino sugars of adriamycin and (N-methyl)-adriamycin. This is ostensibly due to their much lower concentrations. In order to achieve coupling for the reduced amino sugars of **1** and **1b**, a

saturated solution of fluorescein isothiocyanate was needed. There were a number of problems with this protocol. First of all, it generated a number of possible side reactions for the isothiocyanate. It also made HPLC detection of the coupled amino sugars difficult. Finally, the yields of coupling to the amino sugar were consistently below 50%. Although these technical difficulties may have been overcome, the strategy was ultimately scrapped due to the development of a detection assay using GC-MS.

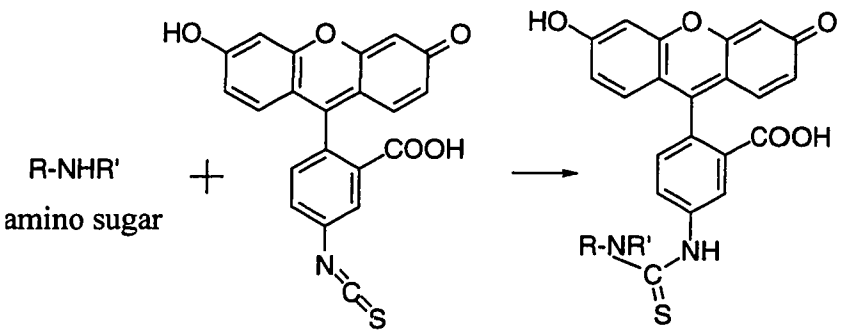

fluorescein isothiocyanate

fluorescein thiourea

Scheme 4. Coupling of amino sugars to fluorescein isothiocyanate. Although this strategy looked promising, because of the development of the GC-MS assay it was ultimately abandoned.

Development of the GC-MS assay

The development of a GC-MS assay was based on a reported study of the separation and quantification of a mixture of sugars. Previously, a mixture of 18 different carbohydrates, including three amino sugars, were separated and quantified by gas chromatography - mass spectrometry (GC-MS).(*63*) The procedure for reduction and preparation of these amino sugars was based on the reduction and acetylation methodology published by Blakeney et al.(*64*) We decided to see if we could reproduce the assay with two model amino sugars. Using a 50:50 mixture of glucosamine and N-methyl glucamine, we sequentially exposed the amino sugars to saturated borohydride

conditions and acetic anhydride to consume the excess borohydride. This was followed by extraction using methylene chloride. The methylene chloride was then removed by evaporation and the remaining residue was dissolved in acetonitrile and analyzed by GC-MS. Reduced and acetylated glucosamine and N-methyl glucamine were then easily separated and detected by GC-MS (**Figure 6**).

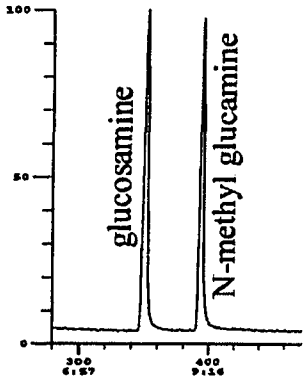

Figure 6. GC-MS analysis of 50:50 moixture of reduced and acetylated glucosamine and N-methyl glucamine.

Given the success of separating the model amino sugars, we set out to see if we could use the same methodology with adriamycin and **1b**. These were also reduced and acetylated in the same manner as the model compounds (**Scheme 5**).

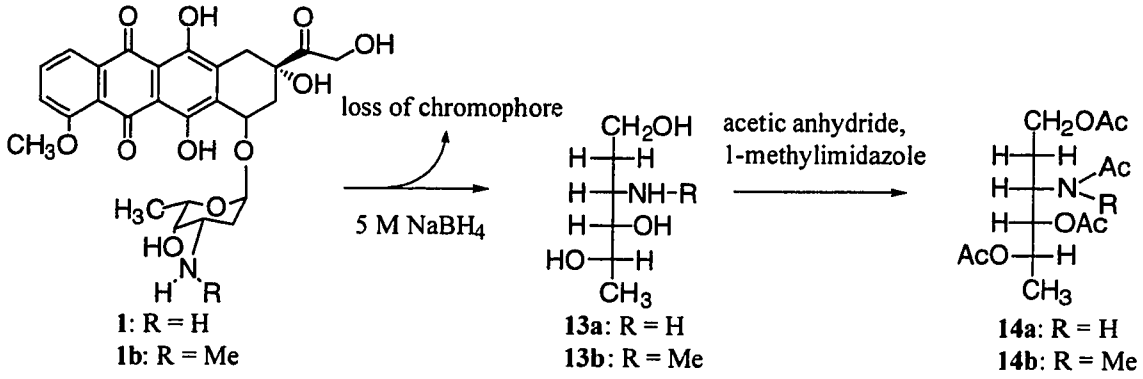

Scheme 5. Scheme for reduction and acetylation of adriamycin and 1b.

Similarly, the very first attempt at detecting and separating the derivatized sugars was successful (**Figure 7**). Mass spectra analysis of **14a** and **14b**, generated from adriamycin and **1b** after borohydride reduction and acetylation, showed three major ions for each (**14a**: m/e 56, 98, 158; **14b**: m/e 70, 112, 172). This is consistent with methylation having occurred at the amino group (**Figure 8**). It seemed that a good method for detection of the two peaks had been found.

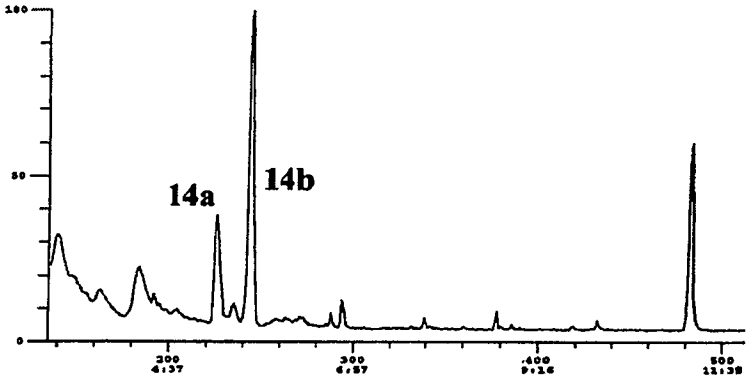

Figure 7. Initial GC-MS analysis of mixture of adriamycin and **1b** exposed to borohydride reduction and acetylation.

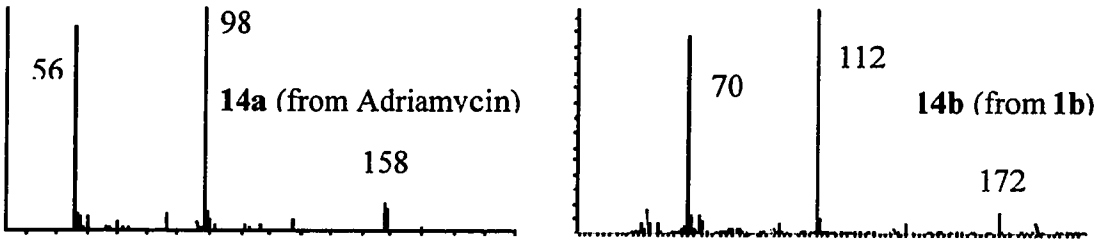

Figure 8. Mass spectrometric analysis of adriamycin and **1b** after borohydride reductions and acetylation.

It quickly became clear, however, that quantification of the peaks was very inconsistent. Using an internal standard of glucosamine, the quantification of **14b** would often vary by as much as 30% in consecutive runs of the same sample. It was

discovered that the way to overcome this obstacle was through the use of single ion monitoring (SIM). With this method, **14a** was detected using m/e of 98, **14b** was detected using m/e of 112, and the reduced and acetylated derivative of glucosamine was detected using m/e of 84 (**Figure 9**). The ion that the mass spectrometer was monitoring would simply change at the appropriate time to detect the appropriate compounds. With this methodology, the precision of the experiment was greatly increased.

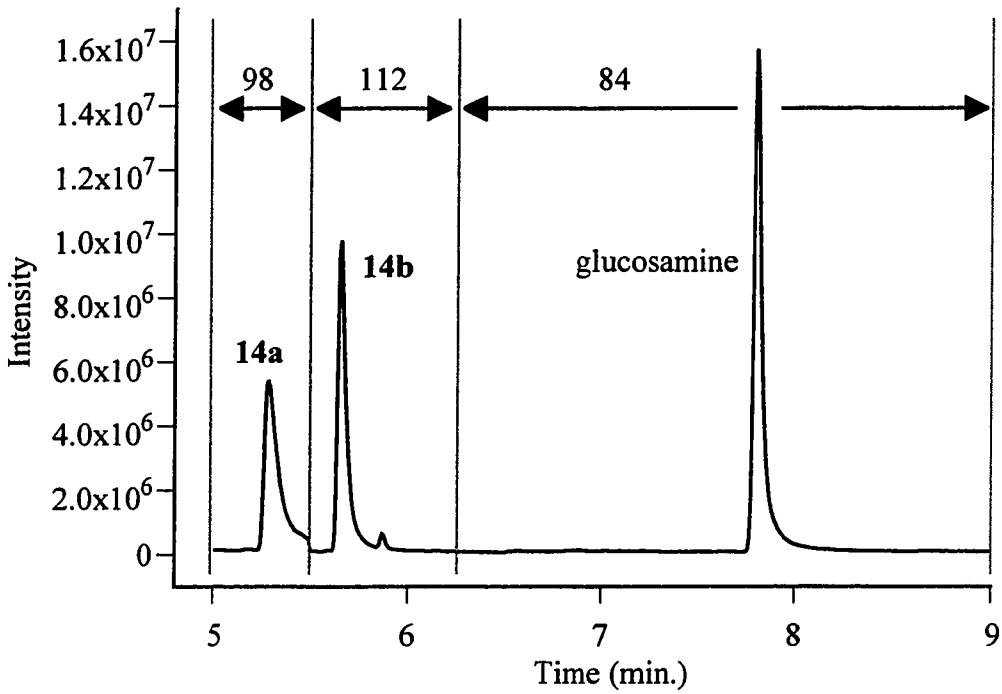

Figure 9. Sample chromatagram of GC-MS experiment in single ion monitoring (SIM) mode. Compounds **14a**, **14b**, and the glucosamine standard are detected by monitoring single ions of 98, 112, and 84, respectively.

There is a linear relationship between the amount of **1b** injected (using glucosamine as an internal standard) and its response on GC-MS (**Figure 10**). Given that we had a developed a good method for detection of the reduced and methylated

amino sugar **14b**, it was time to turn our attention to actual reactions between DNA, adriamycin, and the various activating agents.

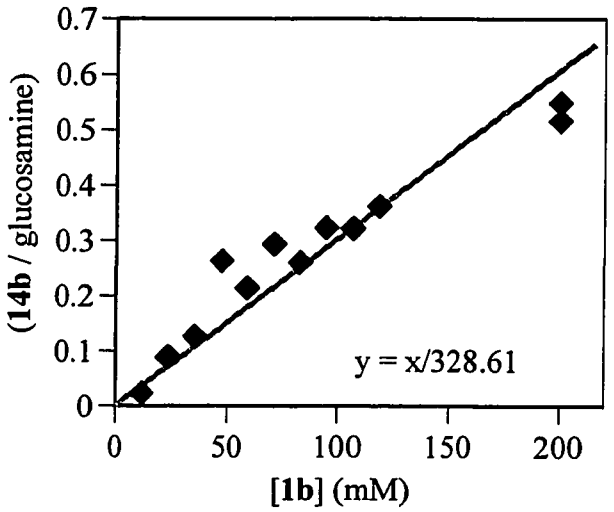

Figure 10. Ratio of areas for peaks for **14b** and glucosamine vs. the [**1b**] (μM). The areas under the peaks for **14b** and glucosamine were determined for known concentrations of **1b** in GC-MS analysis using single ion monitoring. (Linear least squares regression analysis yielded a line with equation: y = x/328.61)

Chapter III. Detection of formaldehyde-mediated adriamycin-DNA crosslinks.

Strategy for detection of lesion 11.

The full strategy for detection of lesion **11** is outlined below (**Scheme 6**). The ability to detect with this method is dependent upon the iminium ion decomposition intermediate being formed on the adriamycin "half" of the unsymmetrical aminal as it decomposes.

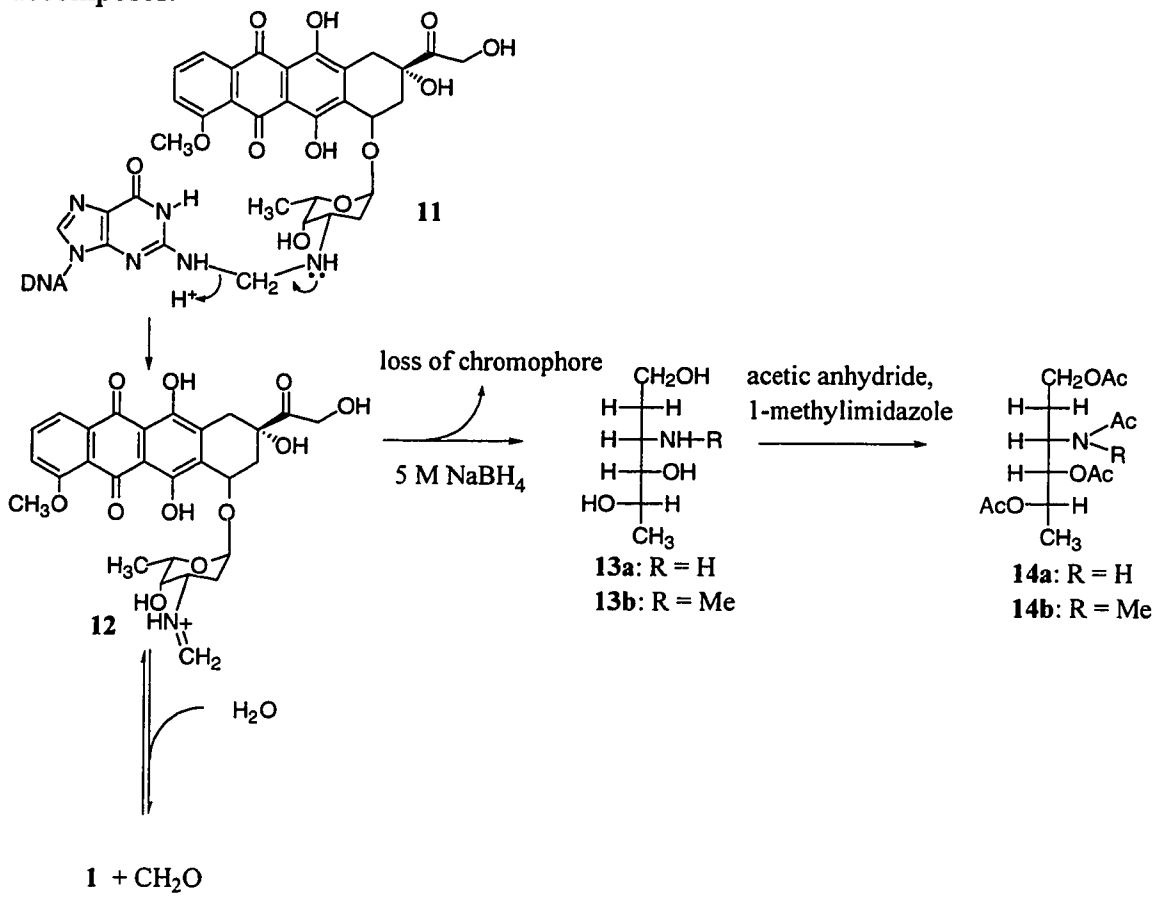

Scheme 6. Strategy for detection of lesion 11 by capturing iminium ion decomposition intermediate 12.

Correlation between Gel and GC-MS Analysis

We assayed mixtures of DNA duplex I, adriamycin, and varying concentrations of formaldehyde using both the DPAGE (**Figure 11A**) and GC-MS (**Figure 11B**) assays. The fraction of DNA that was shifted to the DS DNA band in DPAGE was determined by phosphorimagery. This fraction increased with increasing formaldehyde concentrations, consistent with the idea that formaldehyde is required of DS DNA bands. That the yield of this reaction was saturated at less than 100% DS DNA could reflect dissociation during DPAGE of DNA containing adriamycin covalent adducts or a lower stability towards dissociation of DNA containing certain adriamycin adducts in a structurally heterogeneous mixture. The concentration of **14b** in these same reaction mixtures was determined by GC-MS. Quantification of [**14b**] was performed in all GC-MS experiments by using the least-squares regression line for the N-methyl adriamycin standards versus its GC-MS response. The error bars in GC-MS experiments represent the 95% confidence limits in the value of the slope of that line. Similar to the amount of DS DNA in DPAGE, the concentration of **14b** also rose with increasing formaldehyde concentration, saturating at roughly 1.2 adducts per DNA duplex. Control experiments did not detect any **14b** when DNA is removed from the reaction mixture (data not shown). Given that the reaction mixtures contained no more than 2.0 adriamycin molecules per duplex DNA, the lower limit for the efficiency of this indirect detection method is 60%.

If every covalent linkage of adriamycin to a DNA duplex resulted in production of DS DNA in the DPAGE assay, one would predict that under single hit conditions the concentrations of DS DNA and covalent lesions would be identical at each formaldehyde concentration. In other words, a plot of [**14b**] vs. DS DNA would be linear with slope 1.0. In fact, [**14b**] is roughly twice the concentration of DS DNA at low concentrations of CH_2O (**Figure 11C**). One interpretation is that lesion **11** is formed at guanines at other sequences than 5'-GC, resulting in relatively lower stabilization of the duplex,

without increasing the magnitude of the DS DNA band. Lesion **11** is thus necessary, but not sufficient, for the observation of DS DNA when analyzed by DPAGE.

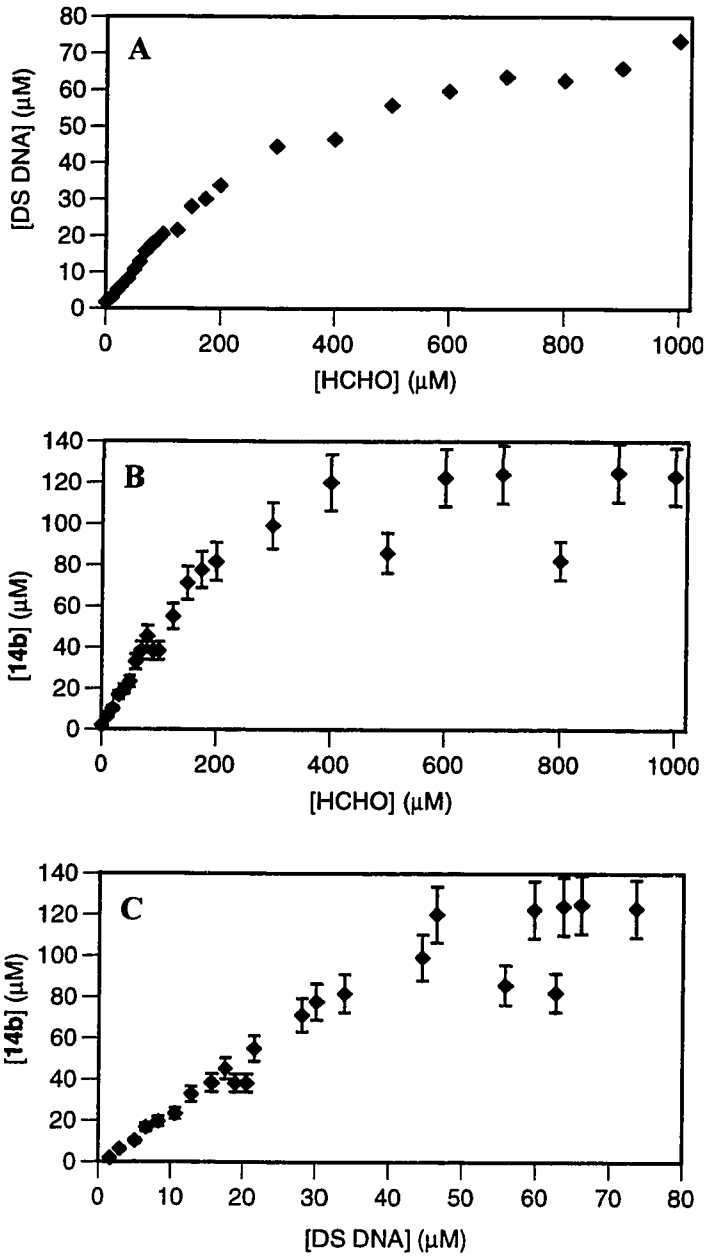

Figure 11. GC-MS and DPAGE analysis of CH_2O-activated lesion formation. Concentrations of DNA duplex I and adriamycin were 100 μM and 200 μM, respectively. (**A**) [DS DNA] determined by phosphorimaging vs. [CH_2O] (μM). (**B**) Concentration of **14b** determined by GC-MS vs. [CH_2O] (μM). (**C**) [**14b**] vs. [DS DNA] for each sample.

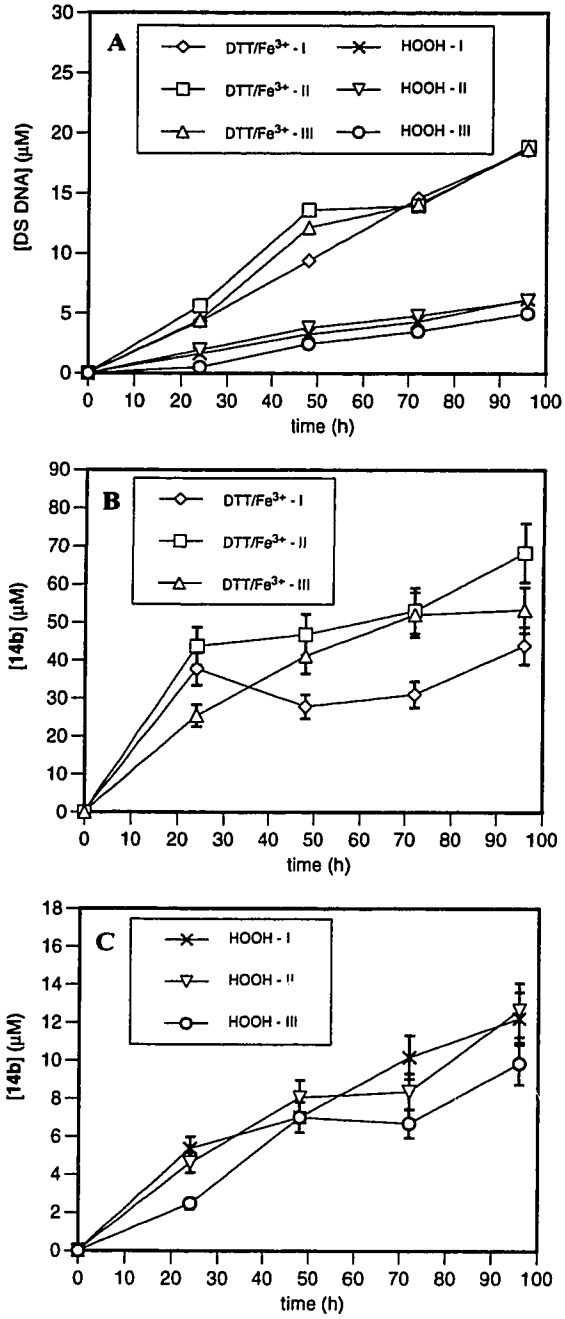

Figure 12. DPAGE and GC-MS analysis of DTT/Fe^{+3} and H_2O_2 activated lesion formation. Concentrations of DTT and Fe^{+3} were 7 mM and 40 µM, respectively. The concentration of H_2O_2 was 5 mM. Each reaction was done in triplicate (I, II, and III) and aliquots were taken every 24 hours. (**A**) [DS DNA] determined by phosphor-imaging for both DTT/Fe^{3+} and H_2O_2 activation. (**B**) [**14b**] determined by GC-MS for DTT/Fe^{+3} activation. (**C**) [**14b**] determined by GC-MS for H_2O_2 activation.

A similar series of experiments was conducted using DTT/Fe^{3+} or H_2O_2 as the activating agents. DNA duplex I (100 μM) was incubated (same buffer conditions) in the dark at 37 °C with adriamycin (200 μM), which was activated by either DTT/Fe^{3+} or H_2O_2. The progress of each reaction was analyzed using both DPAGE and GC-MS. DPAGE showed a gradual increase with time in the amount of DS DNA for either DTT/Fe^{3+} or H_2O_2 (**Figure 12a**). Consistent with DS DNA detected by DPAGE having its origin in **11**, **14b** could be detected and quantified by GC-MS for each of the time points (**Figures 12b** and **12c**). Formation of **14b** required both the activating agent and adriamycin (data not shown).

The correlation of the amounts of **14b** with DS DNA for both DTT/Fe^{3+} and H_2O_2 at various time points is shown (**Figures 13a** and **13b**), respectively, overlaid with the data for formaldehyde at various concentrations. For the DTT/Fe^{3+} activation, there is a significantly larger amount of **14b** found per DS DNA than was the case for formaldehyde. It is important, however, that there is at least as much **14b** detected in each case to cause the amount of DS DNA seen. In other words, some lesions that yield **14b** in the GC-MS analysis in the DTT/Fe^{3+} activation appear not to stabilize DS DNA against denaturation in DPAGE. It may be that reductive methylation of adriamycin that does not involve intermediate **11** is enhanced under these reaction conditions. **14b** is formed in mixtures containing $NaBH_4$, DTT, adriamycin, and CH_2O (data not shown). When DTT was omitted, the level of **14b** fell below the detection limit of the assay. In these control experiments, approximately one-quarter of the quantity of **14b** needed to account for the deviation from the CH_2O data was seen. This control is quite imperfect, though, because DNA is known to bind adriamycin very tightly, potentially altering its ability to interact with DTT. There are other potential reasons for the detection of elevated **14b** levels in the DTT/Fe^{3+} reactions. These include: i) the presence of Fe^{3+} affects the sequence specificity of the formation of lesion **11** or decreases the duplex

DNA's ability to resist denaturation; ii) adriamycin which has been oxidized in a Baeyer-Villiger fashion forms a lesion similar to **11**, but is not as resistant as **11** to denaturation. In contrast, the amount of **14b** detected per DS DNA at each time point was for H_2O_2 activation essentially identical to that seen with formaldehyde. For both DTT/Fe^{3+} and H_2O_2 activation, the correlation between the levels of **14b** with DS DNA is consistent with **11** being the cause of the appearance of DS DNA bands.

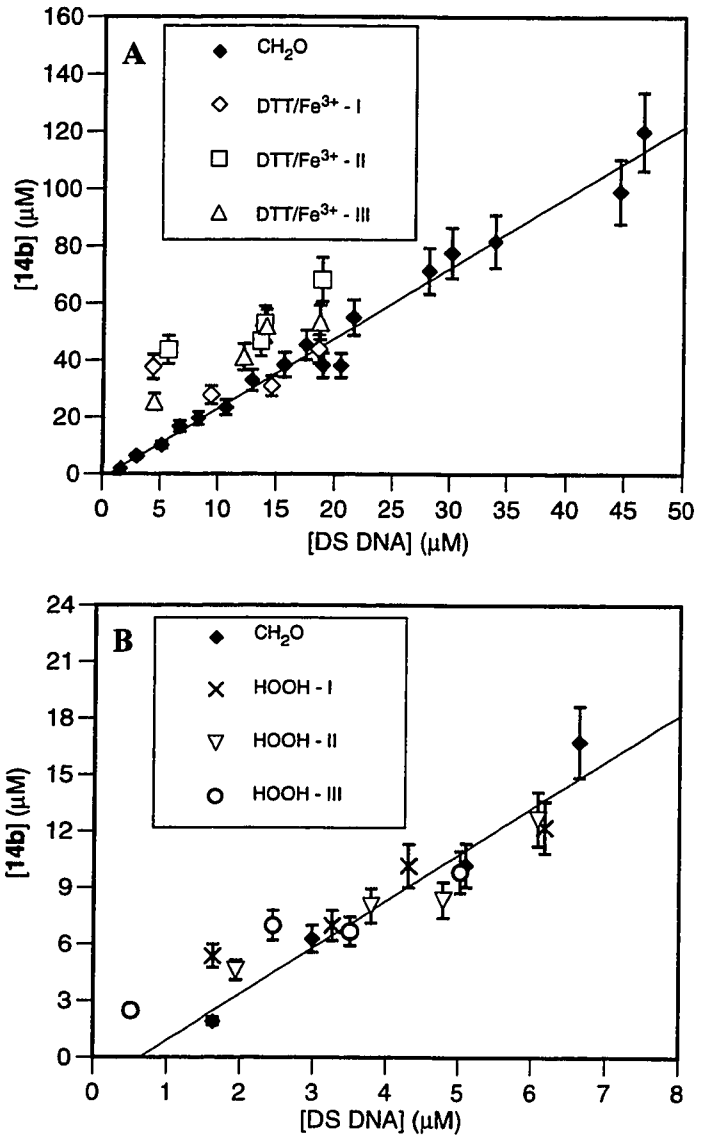

Figure 13. Correlation between DPAGE and GC-MS analyses. [**14b**] vs. [DS DNA] for each time point was plotted for either DTT/Fe^{3+} or H_2O_2 activation and overlaid with the data from the different CH_2O concentrations. (**A**) DTT/Fe^{3+} activation. (**B**) H_2O_2 activation.

Analysis of DS and SS bands by UV/Vis and GC-MS

To provide direct evidence for the presence of lesion **11** in the DS DNA from DPAGE, both single stranded (SS) and DS DNA were isolated and analyzed. DNA

duplex I (100 μM) was incubated (40 mM Tris base, pH 8.0, 50 mM KCl, 3 mM $MgCl_2$, 0.1 mM EDTA) in the dark at 37°C for 96 h with adriamycin (200 μM) which was activated by either DTT/Fe^{3+} or H_2O_2. After ethanol precipitation, the samples were purified by DPAGE. The material eluted from the SS and DS bands was analyzed by UV/Vis spectroscopy (**Table 1**). DNA was enzymatically digested prior to this analysis in order to avoid the hypochromic effect associated with intercalation and allow accurate determination of the concentration of adriamycin.(*65*) For the DS DNA from either DTT/Fe^{3+} or H_2O_2 activation, 1.4 and 1.1 mole equivalents of adriamycin were found per duplex DNA, respectively. For the SS bands, the level of adriamycin was below the level of detection.

Table 1. UV/Vis and GC-MS analysis of excised SS and DS bands.

Sample	[adriamycin][a]	[DNA][a]	[**14b**][b]
H_2O_2 - DS band	244 μM	220 μM	176 μM
H_2O_2 - SS band	<10 μM	283 μM	3.8 μM
DTT/Fe^{3+} - DS band	272 μM	198 μM	185 μM
DTT/Fe^{3+} - SS band	<10 μM	237 μM	5.3 μM

[a]Determined by UV/Vis.
[b]Determined by GC-MS.

On reduction, DNA from the DS band (but not the SS band) afforded roughly the expected yield of **14b** determined by GC-MS (**Figure 14**). **14a** detected by GC-MS for the DS DNA presumably originates by a combination of **11** that has degraded during

the elution from gel slices and adriamycin that remained noncovalently intercalated in the DNA duplex on the gel. Extremely low levels of **14a** and **14b** are detected in the SS band region. That virtually all of the lesion **11** is in the DS DNA region and in levels which are nearly commensurate with the amount of DNA duplex I provides further evidence for this lesion being the cause of the DS DNA observed by DPAGE.

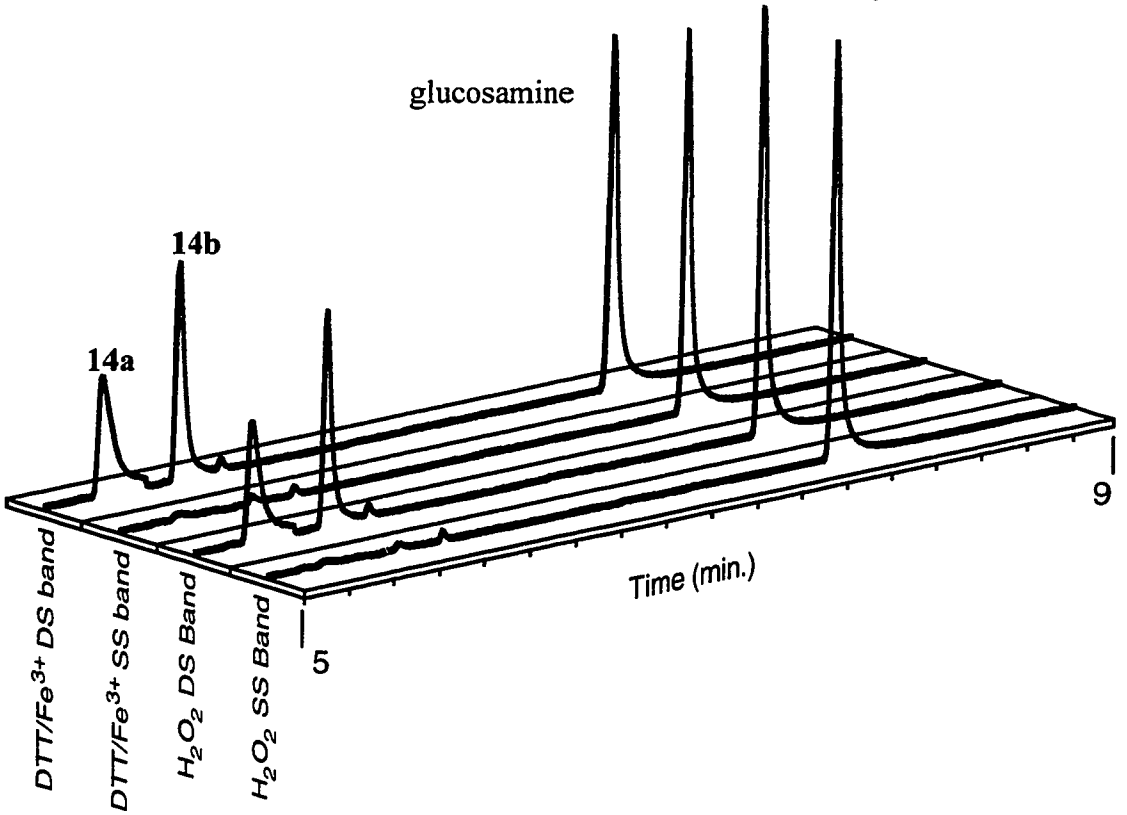

Figure 14. GC-MS chromatagrams of excised SS and DS bands for both DTT/Fe^{3+} and H_2O_2 activated reactions between adriamycin and DNA. GC-MS analyses were done using single-ion monitoring (SIM), monitoring **14a**, **14b**, and glucosamine at 98.1, 112.1, and 84.1, respectively. Chromatagrams were normalized using the integrated area of the internal standard, glucosamine.

Lesion 11 causes DS bands

These results provide further strong support for the conclusion of Koch and co-workers(*53, 54*) that the DS DNA observed by Phillips and co-workers(*48*) are caused

by lesion **11**, and not a true covalent interstrand cross-link. First, it has been shown by DPAGE that activation of adriamycin by DTT/Fe^{3+}, H_2O_2, or CH_2O leads to DS DNA bands by DPAGE. Secondly, we provide further structural evidence for the presence of lesion **11** in these DNAs by detection of methylated adriamycin derivatives resulting from reductive trapping of an intermediate in its decomposition pathway. Thirdly, we show linear correlations between the amounts of lesion **11** and DS DNA observed by DPAGE. Finally, we have indirectly demonstrated that the DS DNA band (but not the SS band) contains lesion **11** when isolated from the gel.

Sequence preference for formation of 11

It seems reasonable to assume that formation of lesion **11** proceeds through a non-covalent complex of adriamycin and DNA. It has been shown that the preferred DNA sequence at which adriamycin binds non-covalently is either 5'-(A/T)CG or 5'-(A/T)GC.(*66*) The chromophore is intercalated between either the CpG or GpC steps and the daunosamine sugar lies in the minor groove next to the AT base pair. Neither of these two complexes, however, is competent to progress to lesion **11**, because the formaldehyde-mediated coupling can occur only when the daunosamine moiety is in close proximity to a dG residue. As such, we presume that these DNA sequences which exhibit higher affinity for non-covalent binding of adriamycin compete with the lower affinity sequences at which covalent binding is ultimately observed. The latter point has not been experimentally investigated.

We still have not resolved the contradiction inherent in the strong preference for DNAs containing $[5'\text{-d(GC)}]_2$ to yield DS DNA bands on DPAGE, despite the observation that formaldehyde-mediated coupling of daunorubicin to guanine can occur in any sequence. Either one or both of two explanations could account for the requirement of $[5'\text{-d(GC)}]_2$ for the generation of DS bands on DPAGE, Either (a) lesion

11 forms preferentially at the sequence [5'-d(GC)]$_2$ or (b) DNAs containing lesion **11** and the sequence [5'-d(GC)]$_2$ are more resistant to denaturation. Our data support the first explanation but provide no information on the second.

Although Chaires observed that the formaldehyde-mediated coupling of daunorubicin to guanine occurred in any sequence, the conditions for this coupling involved much higher concentrations of CH_2O (at least 500-fold) than were used in the experiments reported here.(*56*) It seems possible that at such high concentrations the differences in reactivity of guanines in different sequence contexts would be masked. We have observed that small changes in DNA structure can effect the rate of formation of lesion **11**. GC-MS experiments reveal that lesion **11** (as detected through **14b**) is formed at least 50-fold more efficiently at the sequence [5'-d(GC)]$_2$ relative to either 5'-d(GC) • 5'-d(IC) or [5'-d(CG)]$_2$ (**Figure 15**). Deoxyinosine (dI) is an analog of deoxyguanosine that lacks the exocyclic amino group. In these experiments involving dI, DNA duplexes **II**, **III**, **IV**, and **V** were exposed to a constant concentration of adriamycin and varying concentrations of formaldehyde for a 24-hour period. After ethanol precipitation of the samples, they were reduced, acetylated and subjected to GC-MS analysis. The sequence containing [5'-d(GC)]$_2$ clearly causes the detection of the most **14b.** Although the possibility that borohydride trapping is less efficient in these other sequence contexts can not be excluded, it seems likely that the rate of formation of lesion **11** is greatest at the dinucleotide sequence [5'-d(GC)]$_2$.

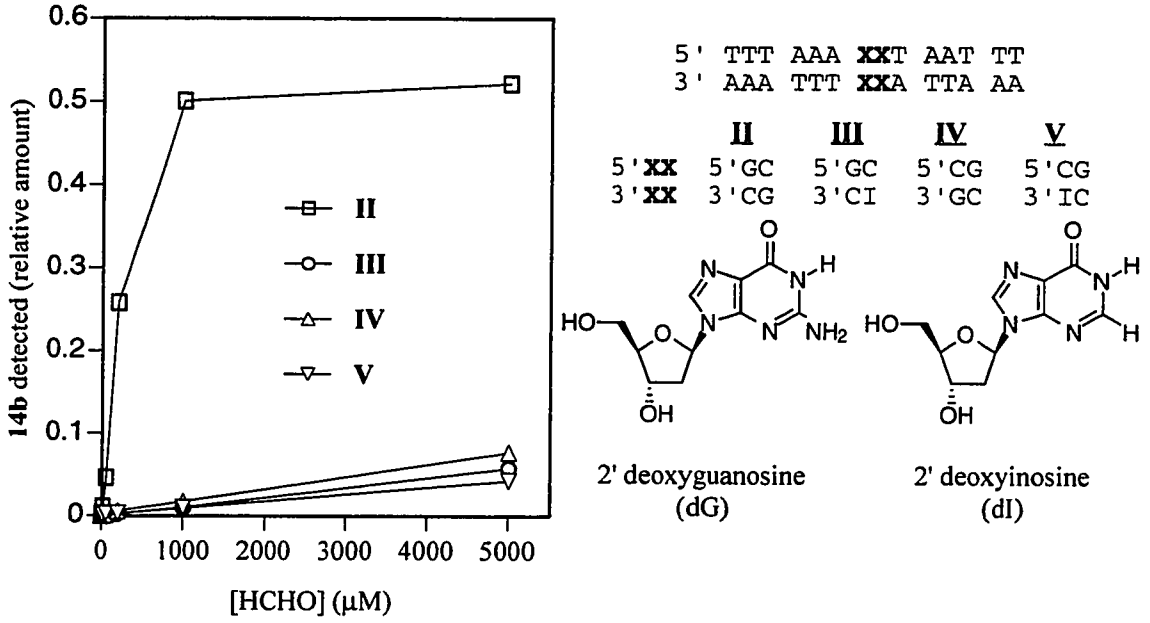

Figure 15. Relative amounts of 14b detected by GC-MS for DNA duplexes **II**, **III**, **IV**, and **V**. DNA duplexes **II**, **III**, **IV**, and **V** (50 μM) were incubated (40 mM Tris base, pH 8.0, 50 mM KCl, 3 mM $MgCl_2$, 0.1 mM EDTA) in the dark at 37°C with adriamycin (50 μM) and various concentrations of formaldehyde for 24 hours (0-5000 μM). These samples were then ethanol precipitated, reduced by borohydride, acetylated, and analyzed by GC-MS.

Causes of seqence specificity

Koch has suggested that a hydrogen bond between the 9-OH of adriamycin and N2 of dG on the non-alkylated strand is required for the observation of the DS DNA bands, acting as a "virtual cross-link". Given the greatly diminished amounts of **14b** detected in the duplex 5'-d(GC) • 5'-d(IC) compared to $[5'\text{-d(GC)}]_2$, it seems reasonable that this hydrogen bond is important for formation of lesion **11**. Whether or not this hydrogen bond is important for the resulting resistance of the duplex to denaturation is unclear. It has been determined, however, that 9-OH of doxorubicin contributes approximately 1 kcal/mol to the non-covalent binding of DNA, presumably due to hydrogen bonding.(*34*)

This study demonstrates a serious and potentially general failing of DPAGE analysis as an indicator of covalent DNA interstrand cross-linking, particularly in cases where presumed thermal lability of the cross-link precludes vigorous denaturation of DNA samples. In this system, non-covalent interactions are evidently strong enough to leave the DNA duplex intact under the conditions of DPAGE.

Questions remain as to the biological relevance of the formaldehyde-mediated alkylation of DNA by adriamycin. Several adriamycin derivatives which are known to alkylate DNA have each been shown to be more cytotoxic than the parent adriamycin. These include cyanomorpholino-doxorubicin (**15**),(*67*) 2-pyrrolino-doxorubicin (**16**),(*68*) N-(5,5-diacetoxypentyl)-doxorubicin (**17**),(*69*) and doxoform (**18**).(*70*) Each of these compounds has a masked aldehyde functionality through which it in principle could alkylate DNA, bypassing the need for formaldehyde. The greater potency of these derivatives relative to adriamycin suggests that formaldehyde-mediated alkylation or related reactions may be important.

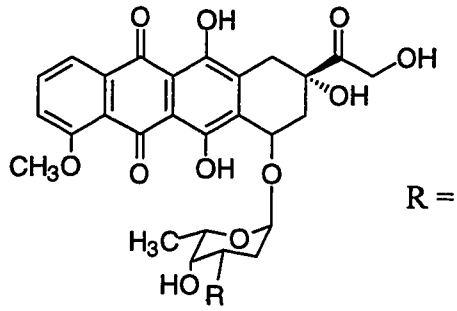

R = 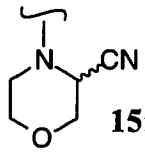

15: cyanomorpholino-doxorubicin

R = 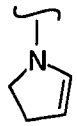

16: 2-pyrrolino-doxorubicin

R = 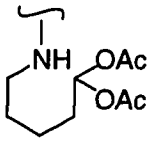

17: N-(5,5-diacetoxypentyl)-doxorubicin

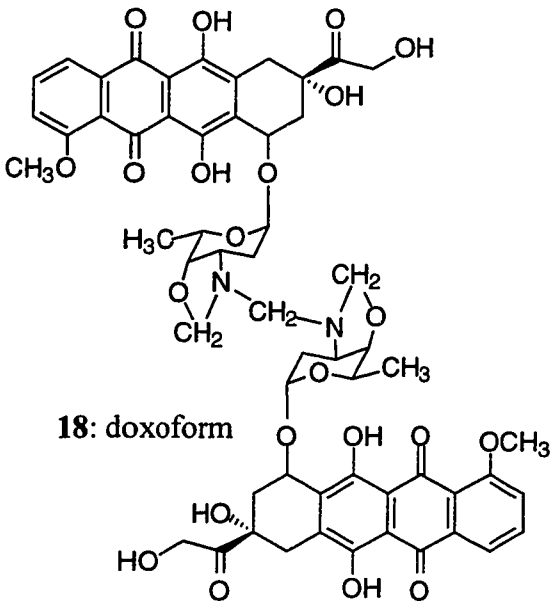

18: doxoform

Summary

The GC-MS assay described herein opens avenues to further investigate the sequence specificity with which **11** forms in DNA. The specific kinetic and thermodynamic parameters of the formation of **11** can be determined using this assay, as well as the effects of adjacent nucleotide bases. Similarly, the GC-MS assay could potentially be used for quantification of **11** in biological systems. In sum, this study has

helped to further define areas of importance in adriamycin's interactions with DNA. It is hoped that this information can be used to develop more effective treatments for cancer.

Chapter IV. HMG proteins, cisplatin, and platination of DNA

Introduction to HMG proteins.

HMG proteins are a class of DNA-binding proteins that contain one or more HMG boxes, a conserved sequence of amino acids 80-85 residues in length. The first discovered HMG protein, HMG1, was named thus because of its high electrophoretic mobility on sodium-dodecyl-sulfate polyacrylamide gels (SDS-PAGE) – "High Mobility Group." Tjian and co-workers recognized that there were more than one of this type of protein when they saw that the HMG box was also in human Upstream Binding Factor (hUBF).(*71*)

Several HMG proteins are known now, including HMG1, HMG2, lymphoid transcription factors TCF-1 and LEF-1, the fungal mating-type mat-Mc and MATA1, the mammalian sex-determining SRY, and the nucleolar transcription factor UBF.(*72*) These proteins can either have single or multiple HMG boxes.(*72*) The general structure of an HMG box is believed to contain three alpha helices situated in an L-shaped structure (**Figure 16**).(*72b*)

Fig. 16. General structure of HMG box. Figure taken from reference.(*72b*)

Similar to a number of proteins, HMG proteins bind to DNA. What is unique about this class of proteins, however, is that several HMG proteins bind to DNA in a structure-specific fashion, meaning that they bind to certain architectures in DNA, not specific sequences. One of the most studied architectures that is known to bind HMG proteins is the four-way junction (4wj) of DNA.(*73*) The four-way junction, also called the Holliday junction, is illustrated below (**Figure 17**). Similarly, it has been shown that some HMG proteins bind tightly to DNA's containing cisplatin intrastrand crosslinks.(*74*)

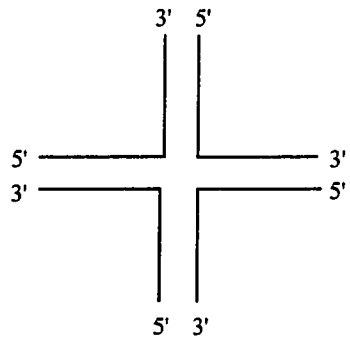

Figure 17. General structure of 4-way junction.

Binding of proteins to DNA

The mechanisms by which proteins bind a specific sequence in DNA are much better understood than those involved in non-sequence-specific binding. For example, in binding a specific sequence, hydrogen bonding patterns of nucleotides often correlate with specific amino acid sequences. The mechanisms by which less evident features can guide binding in non-sequence-specific recognition are not as well understood.(*75*) The main reason for this is that there are several technical difficulties associated with studying non-sequence-specific recognition. The lower binding constants, as well as

competition between multiple binding modes, make the traditional methods of study, gel shift assays, NMR and x-ray crystallography, much more difficult.(*75*)

HMG proteins may be a good way of bridging the two systems of sequence-specific and non-sequence-specific binding. Although they do not bind specific sequences, they clearly recognize certain architectures. This makes these proteins an attractive system to study.

xUBF Box1 and initial project goals

The HMG box that was selected for this study was the N-terminal of the five HMG boxes in Upstream Binding Factor 1 from *Xenopus laevix* (xUBF1). It spans residues 100-182 of xUBF and was expressed in *E. coli* (**Figure 18**). The experimental details of the expression and purification of xUBF Box 1 will be found within the dissertation of Ms. Angie Kantola. Like other HMG proteins, there was evidence that the full xUBF protein bound 4wj and cisplatin intrastrand crosslinks.(*76*)

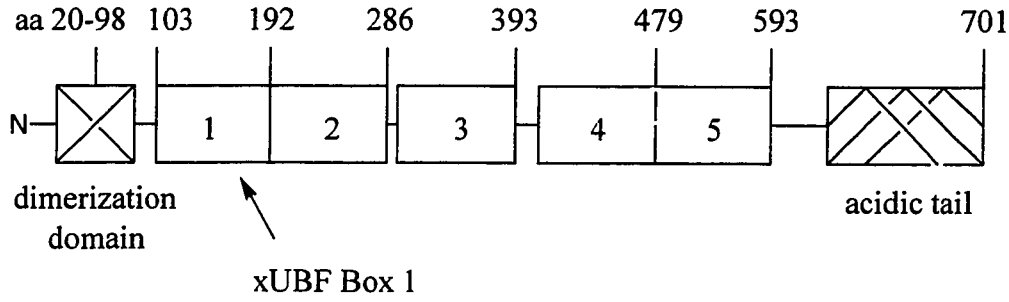

Figure 18. Schematic of full-length UBF from ***Xenopus laevis.*** The HMG box used was xUBF Box 1.

Previous to the research outlined in this dissertation, Dr. Paula Fischhaber developed an NMR-size sample of native and cisplatin intrastrand crosslinked DNA

(duplex **P**). NMR was performed by Dr. Fischhaber and Miss Angie Kantola and used to study the binding of these two duplexes to xUBF Box 1. Each duplex bound the protein with a dissociation constant estimated to be in the micromolar range. The lifetime of the complex was estimated to be in the millisecond range.(*75*) The mode of binding for the platinated and native duplex appeared to be very different upon investigation of the NMR data, but the details of the 3-dimensional structure could not be determined because the equilibrium constant, K_{eq}, was too high. Our goal was to develop a system where the 3-dimensional structure could be determined.

P-Pt

5' TCC TTC TGG TCT CTT
3' AGG AAG ACC AGA GAA

Sequence of platinated sequence previously studied by NMR.

At the onset of this research, there were several initial goals. The first of these was to develop a system where DNA binds to xUBF Box 1 specifically. This means that there is predominately one binding mode and complex between the oligonucleotide and the protein. Several parameters needed be determined. These included the sequence of the DNA, any chemical alterations needed to be made to the oligonucleotide, and the salt conditions. After determining appropriate parameters for this system, it would be studied by NMR, calorimetry, and EPR. Our original goal was to develop oligonulceotides and conditions where specific binding is observed and to investigate this using electrophoretic mobility shift assays (EMSA).

As stated before, 4-way junctions and cisplatin intrastrand crosslinks are potentially good targets for binding of xUBF1. Unfortunately, attempts to examine the binding of HMG proteins to 4-way junctions by NMR had been previously unsuccessful. Presumably, this was due to the large molecular weight of the 4-way

junction needed. Therefore, our starting point was to examine cisplatin intrastrand crosslinks.

Cisplatin

Cisplatin was discovered in the early 1960's when Rosenberg and coworkers were investigating the effect of alternating current on a growing bacterial culture. They observed that the bacteria stopped dividing and grew into long filaments.(*28, 77, 78*) This phenomenon had been observed in bacteria exposed to radiation or alkylating agents, both of which were known to alter chromosomal structure. Rosenberg and coworkers determined, however, that the electricity was not the direct cause of this. When the current was turned off, the aqueous solution maintained its ability to bring about the anomalous bacterial growth. It was determined that platinum was being released from the electrodes as hexachloroplatinate during the process. Hexachloroplatinate, in turn, formed cis-Pt(II)$(NH_3)_2Cl_2$ in the presence of NH_4^+ salts and light. This compound is called *cis*-diamminedichloroplatinum(II) (**19**). It is a square planar platinum (II) compound with the ammonia and chloride ligands on opposite sides of the platinum. This compound, also called cisplatin, was quickly shown to be an effective antitumor agent.

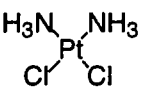

19

Cisplatin is one of the most frequently used anticancer drugs. It is used in combination therapy for tumors of the testis, ovary, head and neck, lung, and bladder.(*2*) The largest obstacles to therapeutic use of cisplatin are the associated nephrotoxicity (kidneys), ototoxicity (ears) and peripheral neuropathy (spinal cord). Toxicity to the kidneys is often the most dose-limiting.(*2*) Similar to adriamycin, the activity of cisplatin almost certainly stems from its interactions with DNA.

Interactions of cisplatin with DNA

Cisplatin essentially forms four types of crosslinks in DNA. These include intrastrand crosslinks at the DNA sequences 5'-GG, 5'-AG, and 5'-GNG as well as interstrand crosslinks at the DNA sequence 5'-GC.(*79-81*) All of these crosslinks are formed between N7 of the purine nucleotides involved and the platinum(II) atom. The 5'-GG intrastrand crosslink is the most commonly formed of these lesions (**Figure 19**).

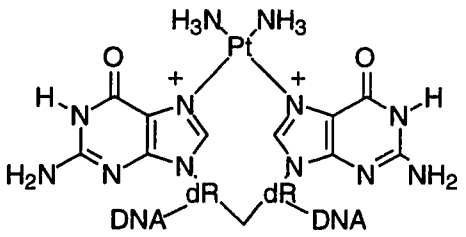

Figure 19. General structure of 5'-GG cisplatin intrastrand crosslink.

Along with being the most prevalent, it is believed that the 5'-GG intrastrand crosslink (ICL) is the most important lesion with regard to the antitumor activity of cisplatin.(*82*) It has also been shown that the 5'-GG ICL is a high affinity site for HMG proteins.(*83-86*) It is believed that the binding of HMG proteins to 5'-GG ICL's shields the lesion from excision repair, eventually disrupting DNA synthesis and leading to cell death. What is important to our research, however, is that cisplatin 5'-GG intrastrand crosslinks have been shown to specifically bind HMG proteins.

Platination and purification of synthetic oligonucleotides

Lippard and coworkers examined a library of nine synthetic 15-mer oligonucleotides, both native and with cisplatin intrastrand crosslinks, for binding to two different HMG boxes, HMG1 domain A and domain B.(*87*) Each member of this

library of 15-mers had a central 5'-GG sequence with a variety of flanking bases (**Table 2**). Lippard and coworkers saw differences in HMG box affinity of up to 2 orders of magnitude within this library, indicating that flanking base composition is an important parameter for protein binding. With this in mind, we set out to synthesize the same cisplatin intrastrand crosslink library and determine the relative affinities of these oligonucleotides to xUBF Box 1.

Table 2. Library of 15-mer oligonucleotides synthesized for platination.

	Sequence Label	N^1	N^2
5' CCT CTC **N1** GG **N2** TC TTC	**A**	A	A
	B	A	T
	C	A	C
	D	T	A
	E	T	T
	F	T	C
	G	C	A
	H	C	T
	I	C	C

Prior to incubation of the single stranded DNA's **A-I**, cisplatin was activated by stirring overnight in aqueous solution. During this process, the chloride ions are replaced by water molecules. Approximately 3.0 O.D. of the single standed DNA 15-mer was then combined with 7.5 μL activated cisplatin [10 mM, 3 equivalents] and incubated in the dark at 37°C for up to 2-5 hours. The platination reactions were monitored and purified using reverse phase high-pressure liquid chromatography (HPLC). Different sequences in the library had different degrees of difficulty in their purification (**Figure 20**). For ease of reference, native strands are referred to by a letter,

whereas the cisplatin intrastrand crosslink of a particular oligonucleotide is the letter followed by "**-Pt**", for example, "**A-Pt.**"

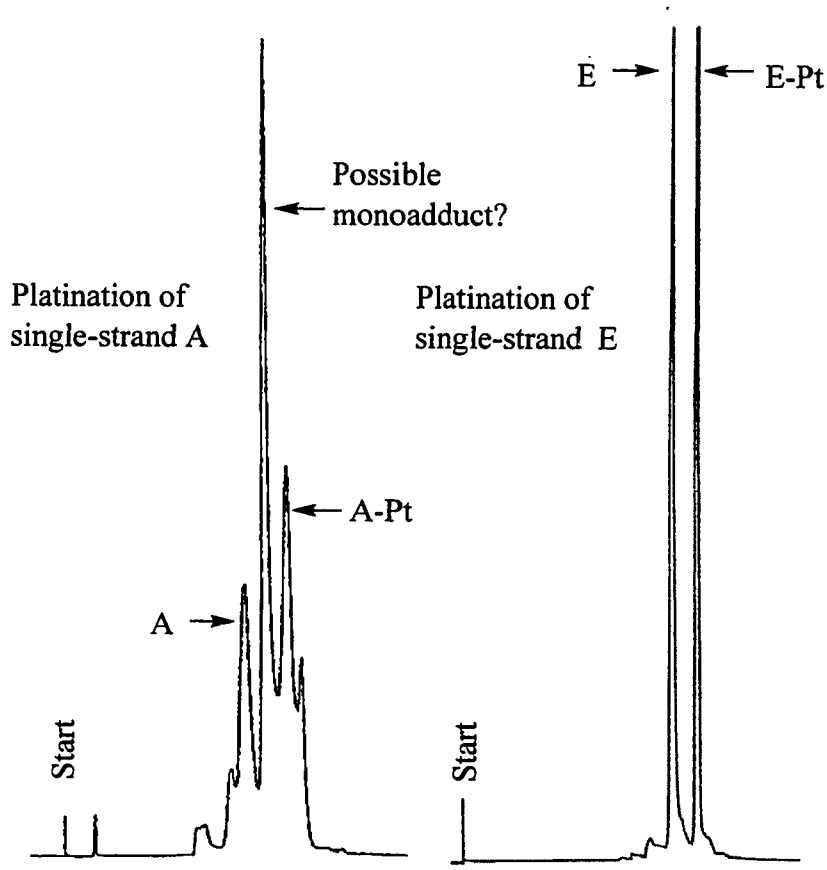

Figure 20. HPLC chromatagrams of platination reactions with single stranded sequences **A** and **E.**

The composition of each peak collected from an HPLC run was determined by two methods. The first of these was enzymatic digestion and subsequent HPLC analysis. Given the presence of only two deoxyguanosines in the sequence, a cisplatin intrastrand crosslink resulted in disappearance of the dG peak (**Figure 21**). The second method of analysis was negative-ion electrospray mass spectrometry. The addition of the crosslink resulted in a net gain of 228 a.m.u (**Figure 22**). Using these two analysis

methods, it was determined that we had successfully prepared the cisplatin intrastrand crosslink for six of the nine potential oligonucleotide sequences.

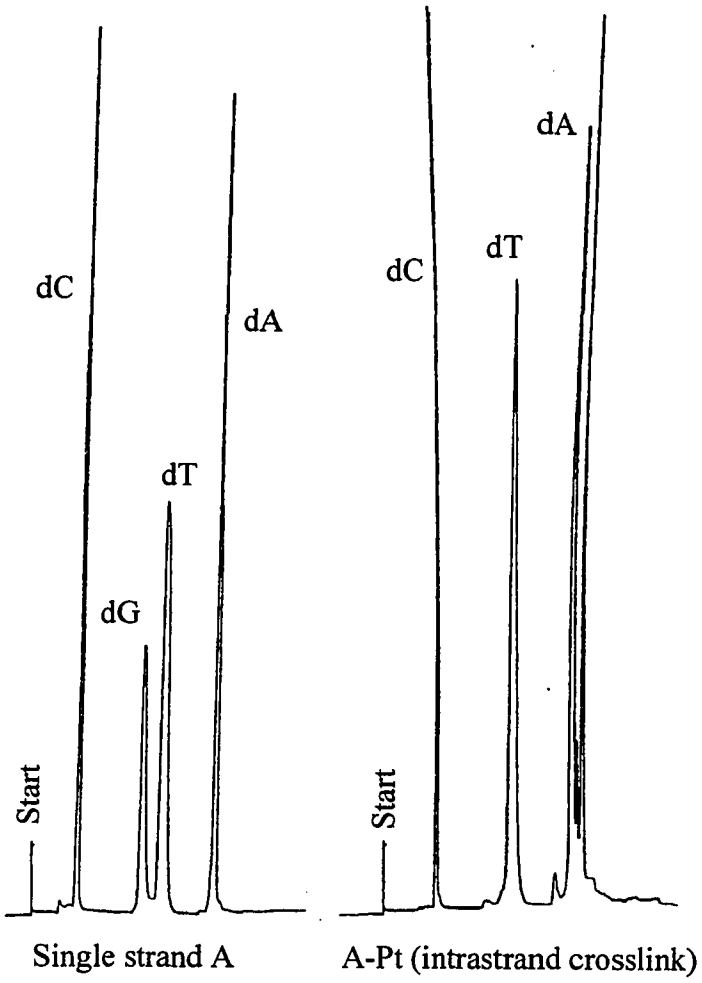

Figure 21. HPLC chromatagrams of enzymatic digests of single-strand oligonucleotide **A** and **A-Pt**. The disappearance of dG in the analysis of **A-Pt** is consistent with the presence of the platinum lesion.

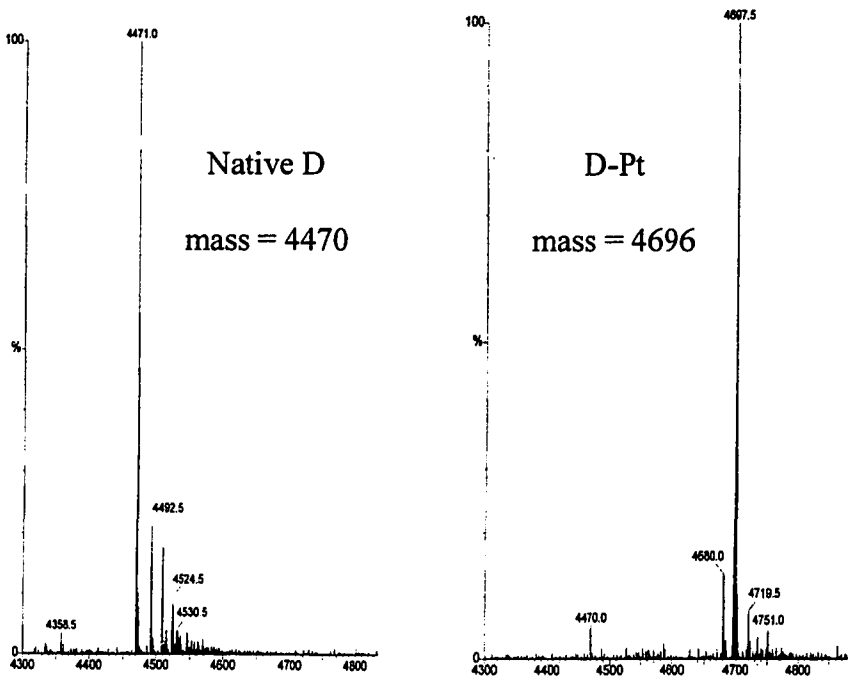

Figure 22. Maximum Entropy calculated spectra of native and cisplatin intrastrand crosslinked DNA sequence **D.** These spectra were calculated based on data from negative-ion electrospray mass spectrometry experiments.

Given that we had established that we could platinate DNA and purify the resulting intrastrand crosslinks, we went on to investigate the binding of xUBF Box 1 to the DNA library. Although only six of the entire library of nine potential oligonucleotides were initially made, this was judged sufficient to begin research into their interactions with xUBF Box 1. It is believed that the three that were not initially made would have been easily purified eventually. We simply wanted to move on to more intellectually challenging and interesting areas of the project. These areas are described in the following chapter.

Chapter V. Binding experiments with HMG

Electrophoretic mobility shift assays

The binding of xUBF Box 1 to the various oligonucleotide sequences was investigated using an electrophoretic mobility shift assay (EMSA). In EMSA, the DNA sequence of interest is radiolabeled and incubated with increasing concentrations of the protein and analyzed by native polyacrylamide gel electrophoresis (PAGE). The conditions of the electorphoresis run are chosen to maximize protein binding; generally this involves colder temperatures. When the DNA is bound to the protein, its movement on the gel is retarded and a slower mobility band is seen (**Figure 23**). The magnitude of each band is then determined and the dissociation constant, K_d, can be calculated.

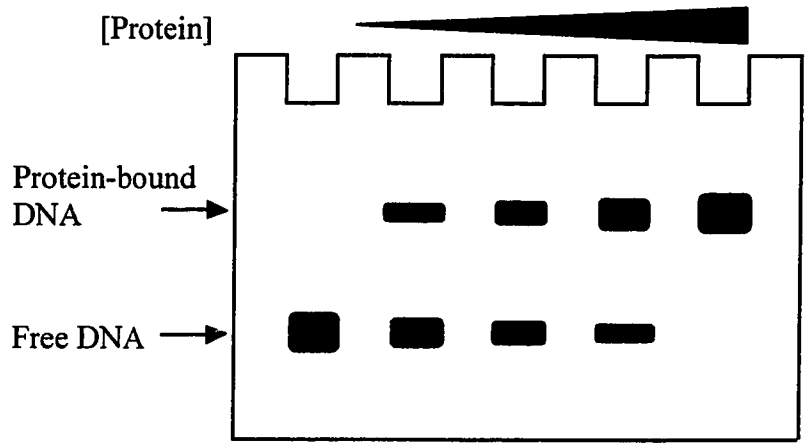

Figure 23. General schematic for electrophoretic mobility shift assay.

Generally, native and platinated oligonucleotides were annealed to 1 equivalent of their complement and then incubated with xUBF Box 1. This incubation was performed on ice, in the dark, with the same buffer conditions used by Lippard and

coworkers (10 mM HEPES, 10 mM $MgCl_2$, 100 mM NaCl, 1 mM spermidine, 2 mg/mL bovine serum albumin, 0.05% Nonidet P-40, pH 7.5).(*87*) After incubation, 50% glycerol is added (resulting glycerol concentration – 12%) to increase the density of the solution and the samples are analyzed by PAGE.

Gel shifts of platinated oligonucleotides

When DNA duplexes **P** and **P-Pt** were investigated previously for binding to xUBF Box 1 by Dr. Paula Fischhaber, no specific binding was seen by EMSA.(*88*) We hoped, however, to use this same EMSA methodology to investigate our newly synthesized library of platinated and native oligonucleotides in order to find a sequence that had tighter binding. Several of the 15-mer oligonucleoides, platinated and native, were investigated for binding to xUBF Box 1 on native PAGE. None of these sequences, however, exhibited specific binding to the protein. With increasing protein concentration, they did not transition nicely from a "free" state to "bound" state on the gel. Instead, at a certain level of protein, they would simply smear up the gel (**Figure 24**). This phenomenon usually indicates non-specific binding between the protein and DNA.

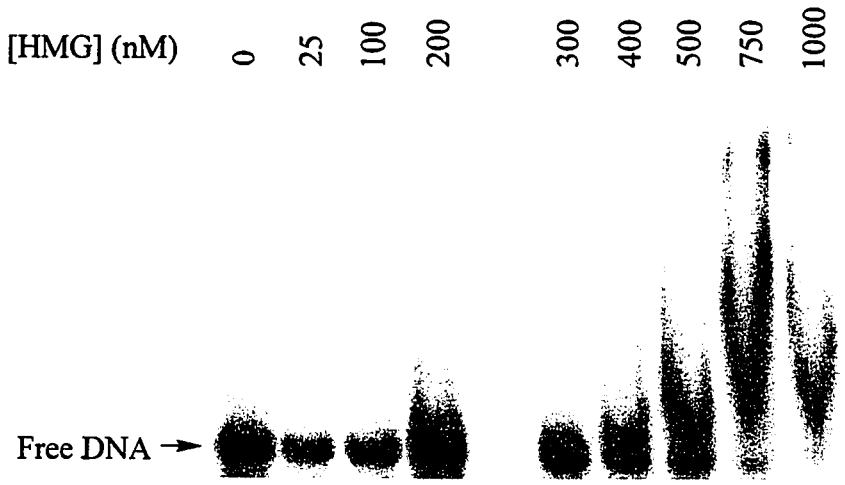

Figure 24. *Binding of duplex* **B-Pt** *to xUBF Box 1.* No specific binding is seen, only a smearing of the DNA on the gel.

It was not entirely unexpected, that none of the 15-mer oligonucleotides, either platinated or native, demonstrated specific binding with the HMG box. During the course of any native gel run, the off rate of the DNA-protein complex might simply be so high that a specific bound complex is not seen. One potential way of circumventing this problem is to make the DNA longer. It has been shown that HMG boxes can more effectively bind longer DNA duplexes.(*89*) We set out to incorporate the 15-mer oligonucleotides into duplexes 50 base pairs in length. This was done in four ways (**Figure 25**). We placed the 15-mer oligonucleotide probe of interest at either the 5' end or in the middle of the 50-mer. We then either assayed these 50-mers as is (assembled), or ligated the different regions of the duplex together.

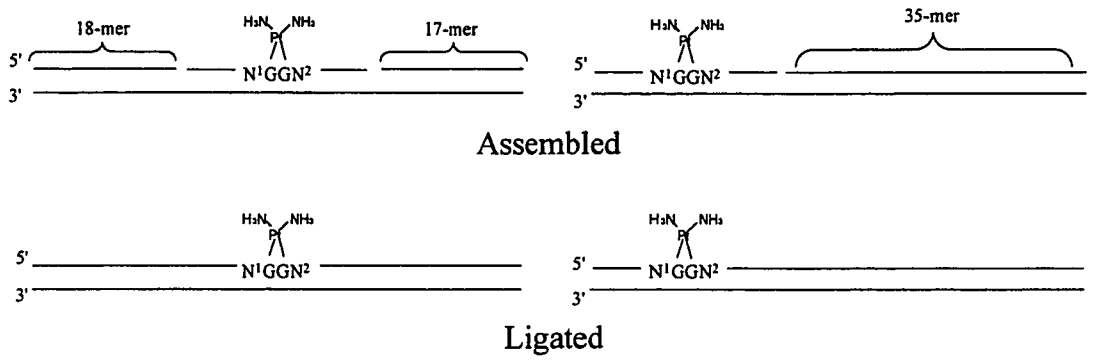

Figure 25. Schematic of assembled and ligated 50-mer oligonucleotides used for assaying binding of platinated and native DNA to xUBF Box 1.

50-mer oligonucleotides are too long to be effectively platinated and purified. This is the reason why they had to be assembled using the previously synthesized 15-mers. Unfortunately, all attempts to shift these 50-mers, either assembled or ligated, resulted in the same "smearing" of the gel seen with the 15-mer oligonucleotides. There was no observed specific binding of the DNA to xUBF Box 1.

Development of competition assay for xUBF binding

As a control to the binding experiments with the 15-mer oligonucleotide library, a 4-way junction was investigated for its binding to xUBF Box 1. The 4-way junction used in these control experiments was developed by Dr. Paula Fischhaber.(*75*) This 4-way junction is composed of two strands, 1sTT2s and 3sTT4s. Each of these has a single hairpin composed of two thymidines (TT), allowing for assembly of the 4-way junction (**Figure 26**).

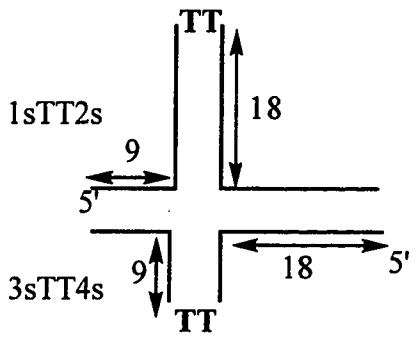

1sTT2s - 5' AGC ACG AGT CCT AAC GCC
AGA TCT GGC **TT** GCC AGA
TCT GGC GTT AGG TGA TAC
CGA TGC ATC GGC

3sTT4s - 5' GCC GAT GCA TCG GTA TCA
GGC TTA CGA **TT** TCG TAA
GCC ACT CGT GCT

Figure 26. Sequence and assembly of 4-way junction DNA (4wj).

Previous experiments showed a K_d of approximately 25-50 nM for this 4-way junction's binding to xUBF Box 1.(*75*) We examined the binding of the 4-way junction to xUBF Box 1 using the same conditions used to investigate the binding of the 15-mer library. Similar to the previous experiments with 4-way junction DNA, we saw a smooth transition from "free" to "bound" DNA (**Figure 27**). The magnitude of each band was calculated using phosphorimagery and ImageQuant™ software. The 4-way junction in this experiment exhibited a K_d of approximately 55 nM, well within range of previously observed values.

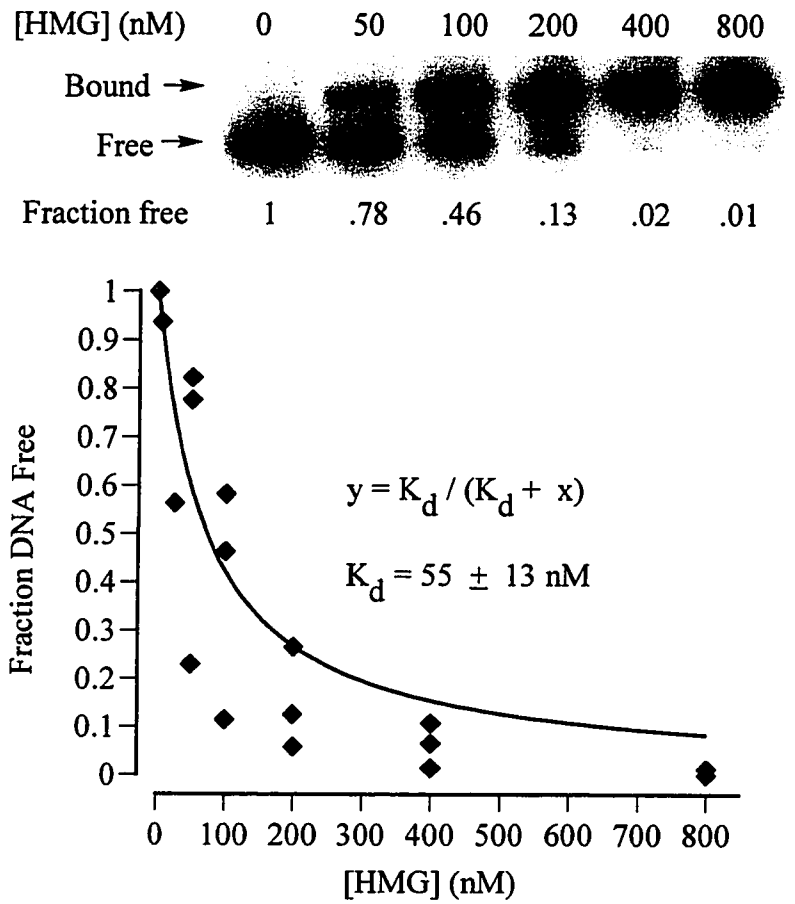

Figure 27. Binding of 4-way junction to xUBF Box 1 and determination of K_d. K_d was determined by combining the data points from three different binding experiments.

The consistent and reproducible binding of the 4-way junction to xUBF Box 1 offered another possible method for examining the binding of the native and platinated duplexes with the protein. It seems possible that the binding between the 15-mer library and 50-mers DNA duplexes to xUBF Box 1 is not tight enough to sustain the complex through the time length of running the gel. Given this possibility, we set out to use the binding of the 4-way junction as a means of assessing the amount of available xUBF Box 1 for binding. The design of the experiment is to keep the concentration of 4wj and xUBF Box 1 constant, titrating in increasing concentrations of the competitor DNA. Assuming that the HMG protein can only bind one nucleotide target at a time, the K_d of any competing nucleotide complex can be determined (**Equation 1**).

Derivation of competition binding equation

There exists a competition between the 4-way junction (4wj) and probe DNA (DNA) to bind xUBF Box 1 (HMG), which can be described using the following equations:

$$[DNA] + [4wj] + [HMG] \underset{k_2}{\overset{k_1}{\rightleftharpoons}} [DNA\text{-}HMG] + [4wj]$$

$$k_4 \uparrow\downarrow k_3$$

$$[DNA] + [4wj - HMG]$$

$$K_{d_{DNA}} = k_2 / k_1$$

$$K_{d_{4wj}} = k_4 / k_3$$

The equation for the dissociation constant for 4wj and HMG is:

$$K_{d_{4wj}} = \frac{[DNA] * [4wj] * [HMG]}{[DNA] * [4wj - HMG]} = \frac{[4wj] * [HMG]}{[4wj\text{-}HMG]}$$

y = fraction 4wj bound

$$\frac{\text{fraction 4wj free}}{\text{fraction 4wj bound}} = \frac{[4wj]}{[4wj\text{-}HMG]} = \frac{(1-y)}{y} = f$$

$$K_{d_{4wj}} = \frac{[4wj] * [HMG]}{[4wj\text{-}HMG]} = \frac{(1-y)}{y} * [HMG] = f * [HMG]$$

HMG_x, y_x, and f_x refer to the values of these variables for a particular value of [competitor DNA] = x. HMG_0, y_0, and f_0 are constants for these values prior to the addition of any competitor DNA.

x = [competitor DNA]

$$K_{d_{4wj}} = f_0 * [HMG_0] = f_x * [HMG_x] \longrightarrow [HMG_x] = (f_0 / f_x) * [HMG_0]$$

$$K_{d_{DNA}} = \frac{[DNA] * [4wj] * [HMG]}{[DNA - HMG] * [4wj]} = \frac{[DNA] * [HMG]}{[DNA\text{-}HMG]} = \frac{x * [HMG_x]}{([HMG_0] - [HMG_x])}$$

$$K_{d_{DNA}} = \frac{x * ((f_0 / f_x) * [HMG_0])}{([HMG_0] - ((f_0 / f_x) * [HMG_0]))} = \frac{x * (f_0 / f_x)}{1 - (f_0 / f_x)} = \frac{x * f_0}{f_x - f_0}$$

Substituting in ($f = (1-y)/y$):

$$K_{d_{DNA}} = \frac{x * ((1-y_0)/y_0)}{((1-y_x)/y_x) - ((1-y_0)/y_0)} = \frac{x * ((1-y_0) * y_x)}{((1-y_x) * y_0) - ((1-y_0) * y_x)}$$

$$K_{d_{DNA}} = \frac{x * ((1-y_0) * y_x)}{y_0 - y_0y_x - y_x + y_0y_x} = \frac{x * ((1-y_0) * y_x)}{y_0 - y_x}$$

$$\frac{y_0 - y_x}{y_x} = \frac{x * (1-y_0)}{K_{d_{DNA}}}$$

$$\frac{y_0 - y_x}{y_x} = \frac{x * (1-y_0)}{K_{d_{DNA}}}$$

$$\frac{y_0}{y_x} = \frac{x * (1-y_0) + K_{d_{DNA}}}{K_{d_{DNA}}}$$

$$\frac{y_x}{y_0} = \frac{K_{d_{DNA}}}{x * (1-y_0) + K_{d_{DNA}}}$$

$$y_x = \frac{y_0 * K_{d_{DNA}}}{x * (1-y_0) + K_{d_{DNA}}}$$

y_0 = 4wj bound (original)

y_x = 4wj bound

x = [comp. DNA]

Equation 1. Equation for determination of $K_{d_{DNA}}$

Using **Equation 1**, a curve-fitting program can be used to calculate values for the K_d of the competitor DNA, as well as the original fraction of 4wj (y_0) bound prior to addition of the competitor DNA. One nice feature about this particular method is that

the concentrations of 4wj and HMG, as well as the K_d of the 4-way junction, do not need to be determined as long as they are kept constant.

Using the competition assay

The first step was to examine the accuracy of the competition assay by competing 4-way junction DNA with itself. Non-radiolabeled (cold) 4-way junction DNA competed with radiolabeled 4-way junction DNA for binding to xUBF Box 1. The concentration of xUBF Box 1 (50 nM) and the concentration of radiolabeled 4wj (<1 nM) were kept constant and mixed with increasing concentrations of cold 4wj DNA. Cold 4wj DNA competed very effectively, with a calculated $K_d = 14 \pm 3$ nM (**Figure 28**). Although this number is slightly lower than the calculated 73 ± 22 nM seen using the electrophoretic mobility shift assay, it is within the same order of magnitude.

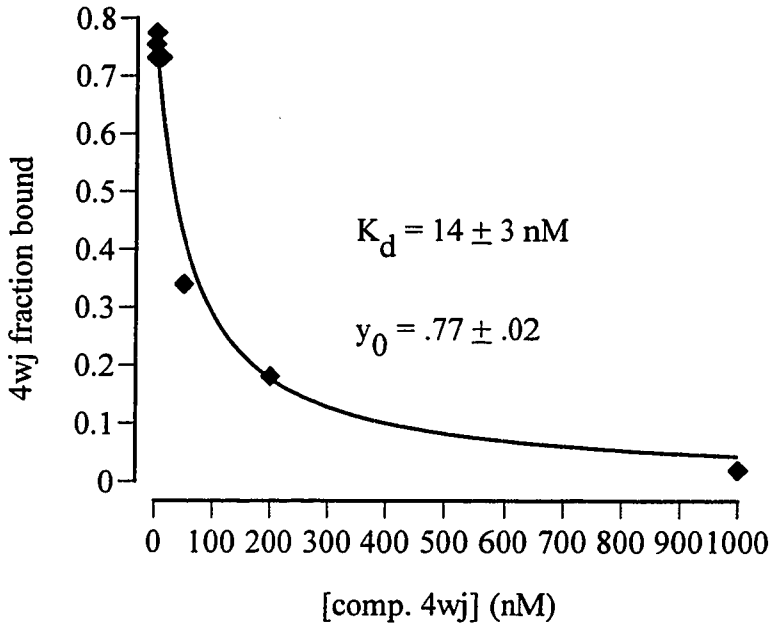

Figure 28. Competition binding assay between radiolabeled and cold 4-way junction DNA with xUBF Box 1.

The library of 15-mer oligonucleotides, native and platinated, were then investigated for their binding to xUBF Box 1 using the competition experiment with 4wj. The three initial sequences examined were duplexes from A-Pt, E-Pt, and P-Pt. The duplex used in previous NMR experiments, **P-Pt**, appears to have a much higher K_d than either of the other two duplexes, **A-Pt** or **E-Pt**. (**Figures 29** and **30**).

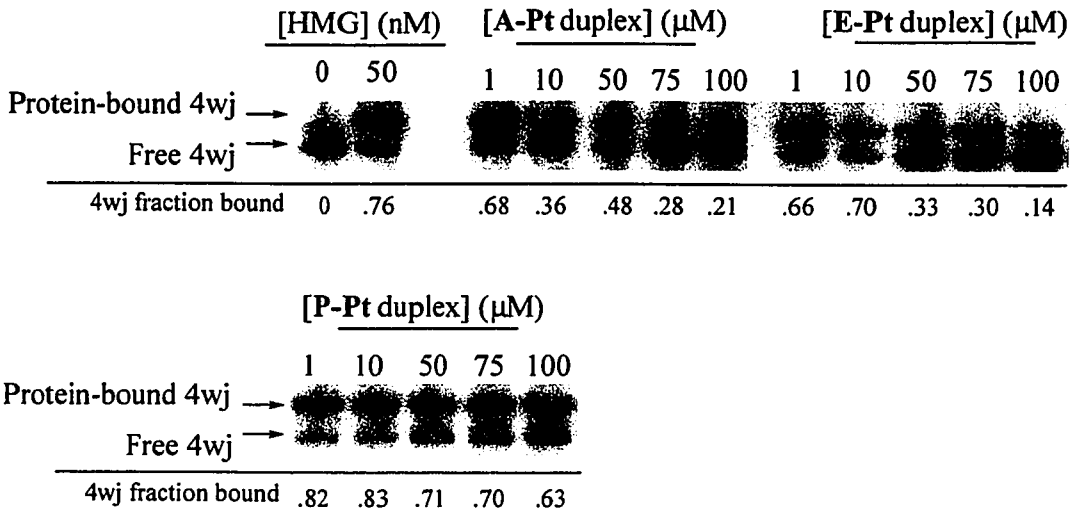

Figure 29. Competition experiments with cisplatin intrastrand crosslinked 15-mer oligonucleotides.

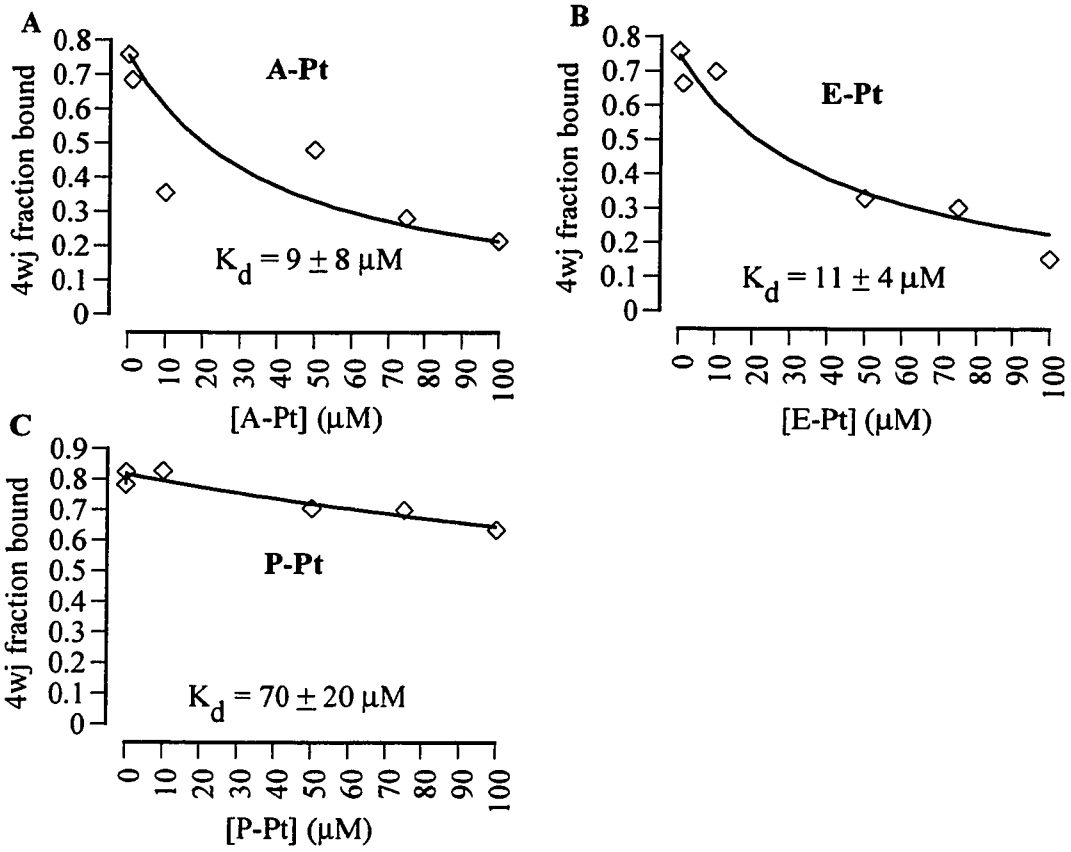

Figure 30. Fraction 4wj bound vs. [competitor DNA] for **A) A-Pt**; **B) E-Pt**; and **C) P-Pt.** Notice that the estimated dissociation constant K_d is much larger for **P-Pt** than that seen for either **A-Pt** or **E-Pt**.

All of the investigated platinated sequences in the 15-mer library based on Lippard's research competed more effectively than **P-Pt** with 4wj DNA for the binding of xUBF Box 1. Each of these platinated duplexes had K_d values of approximately 5-20 μM (data not shown). **P-Pt**, on the other hand, had a reproducible K_d of approximately 70 μM. This was encouraging, as it indicated that any of these sequences would potentially bind better and be a better target for NMR study than DNA duplex **P-Pt.**

Binding of native duplexes and single stranded DNA

The binding of the native duplexes and single-stranded oligonucleotides was also investigated using the competition assay. The native oligonucleotides, in general, bound with approximately the same K_d values as their platinated counterparts. In some cases, they bound more tightly. For example, the native duplex of sequence **D** bound slightly more tightly than **D-Pt** (**Figure 31**).

In general, all of the native 15-mer duplexes and single-stranded oligonucleotides bound with roughly the same range of K_d's as the platinated 15-mers, varying from 5-20 μM. This raises the question as to whether this particular HMG box actually has a higher affinity for platinated oligonucleotides over native duplexes.

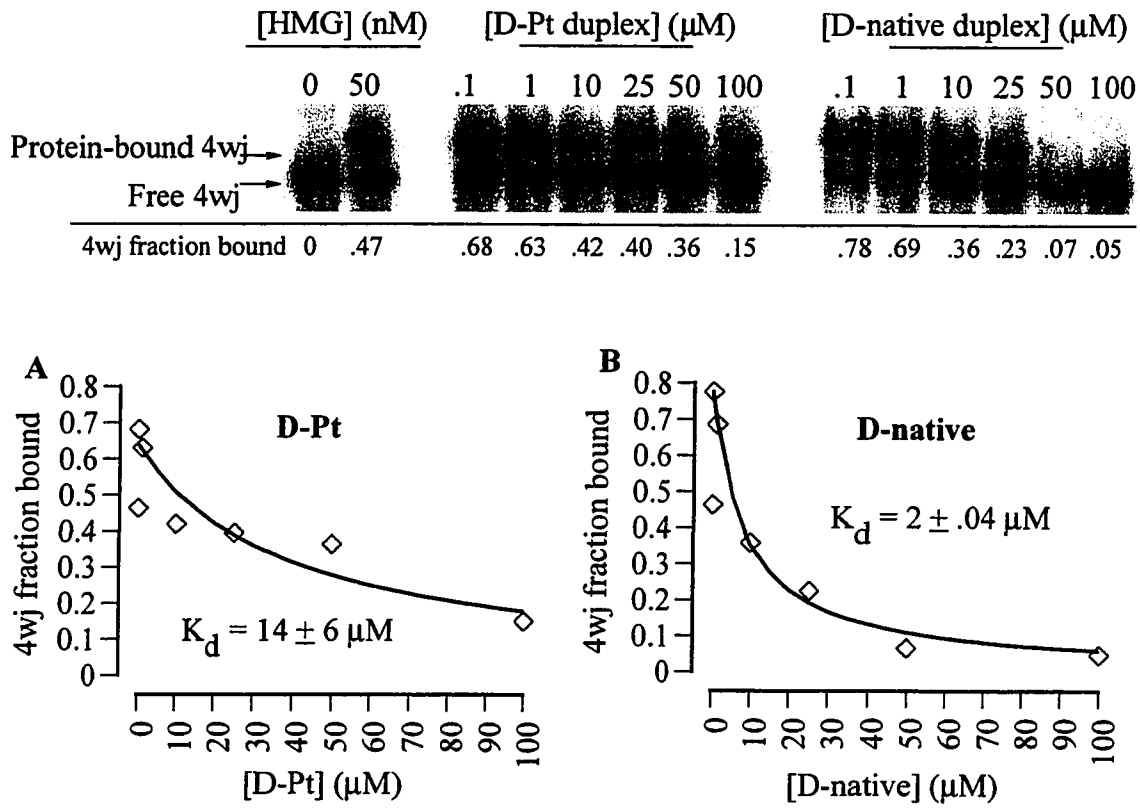

Figure 31. Competition experiments of **D-Pt** and **D-native** duplexes with 4wj binding of xUBF Box 1.

Imperfections in the competition assay

It should be emphasized that the competition assay has several problems. The standard deviation for these K_d values is extremely high and the R^2 values vary widely, between 0.7 and 0.9. Because of this variation, these dissociation constants must be considered only preliminary estimations. To determine accurately the dissociation constants of the native and platinated duplexes, as well as the single-stranded DNA, much more data would need to be collected. The preliminary results of the platinated duplexes, however, are outlined (**Table 3**).

Table 3. Estimated K_d values for platinated duplexes to xUBF Box 1 determined by competition binding assay with 4wj.

	K_d's (μM)	
A-Pt	9 ± 8	
D-Pt	14 ± 6	10 ± 7
E-Pt	11 ± 4	
F-Pt	1 ± 3	2 ± 2
H-Pt	18 ± 14	
P-Pt	70 ± 18	74 ± 11

*Development of NMR-size sample of **D-Pt***

At this point in the study, there was no clear consensus platinated sequence that had the tightest binding to xUBF Box 1. (Although **F-Pt** had the lowest determined K_d, the standard deviation was quite large.) Additionally, the similar affinity of native and single-stranded DNA's to the HMG box raised the question as to whether or not xUBF Box 1 actually has a higher affinity for cisplatin intrastrand crosslinks than for native DNA. Despite this, it was decided to press forward and synthesize an NMR-size sample of **D-Pt**. Although there were no statistically significant differences in the binding of the various platinated duplexes **A-Pt**, **D-Pt**, **E-Pt**, **F-Pt**, and **H-Pt**, each appeared to bind tighter than duplex **P-Pt**. The **P-Pt** duplex binding to xUBF Box 1 had been studied previously by NMR, so it could be used as a baseline to compare any of these potentially tighter binding platinated duplexes. The sequence **D-Pt** was chosen because of its relative ease of platination and purification

D-Pt

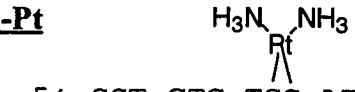

5′ CCT CTC TGG ATC TTC
3′ GGA GAG ACC TAG AAG

An NMR-size sample of platinated **D** synthesized and purified. The presence of the cisplatin intrastrand crosslink was confirmed by HPLC analysis of enzymatic digestion as well as negative-ion electrospray mass spectrometry. The complement to this strand was subsequently synthesized and purified by Ms. Monica Sekharan. Ms. Sekharan also confirmed formation of the duplex. The binding of **D-Pt** duplex to xUBF Box 1 is presently being studied by NMR by Ms. Monica Sekharan and Ms. Angie Kantola. Preliminary results indicate the presence of a single species in both the native and platinated samples. The details of this research will be found in their respective theses.

Binding of nitrous acid crosslink to xUBF Box 1

The 4wj competition assay was used to investigate other DNA duplexes which potentially might have a higher affinity to xUBF Box 1 than cisplatin intrastrand crosslinks. The first of these was the nitrous acid interstrand crosslink. When duplex DNA is exposed to nitrous acid, it forms interstrand crosslinks at the sequence [5'-d(CG)]$_2$. This crosslink was synthesized in the Hopkins laboratory by Eric Harwood and generously donated for investigation of binding to xUBF Box 1. The specific sequence used is illustrated below (**Figure 32**).

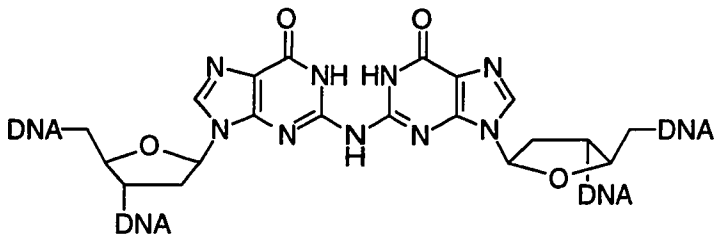

5' GCATCCGGATGC
3' CGTAGGCCTACG

Sequence **NA**

Figure 32. Structure and sequence of nitrous acid crosslink (**NA**).

DNA Duplex NA, both native and with the nitrous acid crosslink, was investigated for binding to xUBF Box 1 using the 4wj competition assay. Surprisingly, the nitrous acid crosslink had a much lower K_d than the native, 3 μM vs. 15 μM (**Figure 33**). The cause of this higher affinity for the nitrous acid crosslink sequence is unclear. The structure of the nitrous acid crosslink is distorted, however, with a widening of the minor groove and extrahelical cytidines.(*90*) This lesion presents another potential DNA target for studying the binding of xUBF Box 1. Attempts to gel shift the nitrous acid crosslink with a standard EMSA were unsuccessful (data not shown).

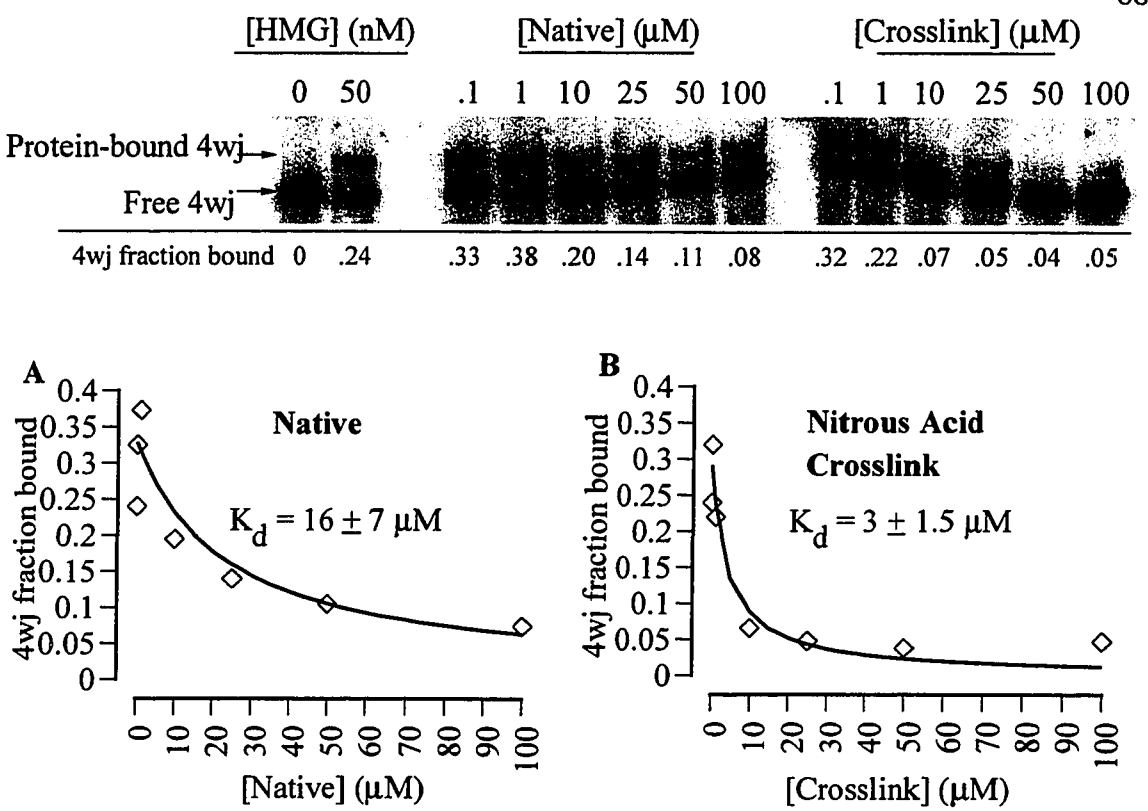

Figure 33. 4wj competition experiments with native and nitrous-acid crosslink versions of sequence **NA.**

Binding of a 34-mer DNA duplex to xUBF Box 1

The binding of a 34-mer DNA duplex to xUBF Box 1 was also investigated using the competition assay (**Figure 34**). The K_d for this 34-mer, 80 ± 40 nM, was much lower than those seen for any of the 15-mer oligonucleotides. It is not clear if this is simply due to its length or some unknown sequence that is contained within the full sequence. It does, however, raise the possibility that longer oligonucleotides, platinated and native, might be better targets for binding.

34-mer duplex:

```
5' AGC TTG GCT GCA GGT CGA CGG ATC CCC GGG AAT T
3' TCG AAC CGA CGT CCA GCT GCC TAG GGG CCC TTA A
```

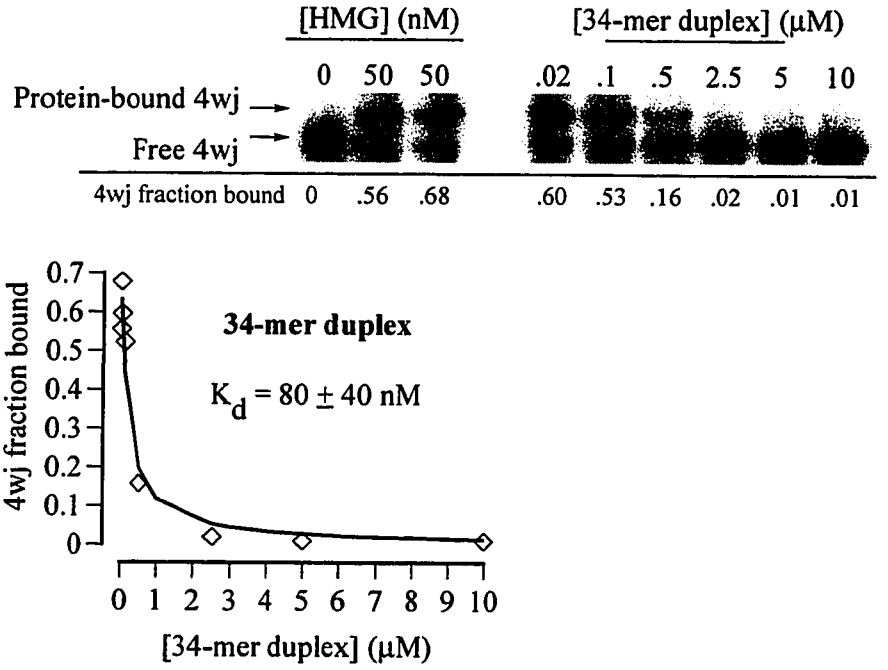

Figure 34. 4wj competition assay with 34-mer duplex.

Concerns about xUBF Box 1

At the onset of this project, it was assumed that xUBF Box 1 would have a higher affinity for cisplatin intrastrand crosslinks than for native DNA. In retrospect, this seems potentially an inaccurate assumption. The competition assay with 4-way junction showed similar K_d values for both native and single-stranded DNA compared to cisplatin intrastrand crosslinks. UBF proteins, which contain multiple HMG boxes, have been shown to have an affinity for cisplatin intrastrand crosslinks.(*91-93*) Despite this phenomenon, there is no literature evidence that xUBF Box 1 by itself has an affinity for these crosslinks. In fact, two variants of human UBF (hUBF) have been shown to have very different affinities for cisplatin-treated DNA.(*94*) This is true despite the fact that four of the five HMG boxes are identical in each. Needed in the

binding experiments with xUBF Box 1 was a control HMG box that is known to bind to platinated oligonucleotides of such short length. One possible control would be HMG1 Box A(*87*)

Summary of DNA-binding by xUBF Box 1

In summary, we have synthesized several platinated 15-mers and investigated their binding to xUBF Box 1 using a competition assay with 4-way junction DNA. The K_d values of the 15-mers in this library ranged from 5-20 μM. The platinated 15-mer previously studied by NMR, **P-Pt**, appears to have a much higher K_d, 70 μM, than the members of this new library. As a result, one sequence, **D-Pt**, has been selected to be studied by NMR. Both the native and platinated versions of sequence **D** were synthesized and NMR is currently being used to study their binding to xUBF Box 1.

We have also made some preliminary investigations into the nitrous acid crosslink and longer DNA duplexes. These areas appear potentially promising for finding a system in which xUBF binds more tightly. In order to determine this, however, more research must be done.

Chapter VI. Experimental Section

Materials and Methods. Materials and their sources were as follows: DNA synthesis reagents, Applied Biosystems; [γ-^{32}P]ATP, DuPont; adriamycin, Sigma; cisplatin, Aldrich; T4 polynucleotide kinase, Amersham or Boehringer Mannheim; 40% 19:1 acrylamide:bis-acrylamide solution, Bio-Rad; acrylamide and bis-acrylamide; GibcoBRL; alkaline phosphatase (calf intestinal), Boehringer Mannheim; and phosphodiesterase I (Crotalus adamanteus venom), Pharmacia. All other reagents were commercial and used as received. Water was purified on a Millipore Milli-Q deionizer. Oligonucleotides were synthesized on an Applied Biosystems Model 392 Synthesizer. Samples were concentrated in vacuo with a Savant SpeedVac speed vacuum concentrator. UV spectra were measured on a Hewlett-Packard 8452A or a Perkin-Elmer Lambda 4a spectrophotometer. All analytical denaturing polyacrylamide gel electrophoresis was conducted on a Hoeffer thermojacketed Poker Face gel stand connected to a Fischer Scientific Model 90 Refrigerated Circulator. Gel loading solution consisted of 5 M urea and 0.5% xylene cyanol. 1 X TBE buffer used for gel electrophoresis was 90 mM Tris/ 90 mM boric acid (pH 7.5) and 1.8 mM Na_2EDTA. Gels were dried using a Bio-Rad Model 583 gel dryer onto Whatman 3M paper; autoradiograms were with Fuji RX film. For phosphorimagery, dried gels were scanned by a Molecular Dynamics 400A PhosphorImager and data analysis was performed using Molecular Dynamics' Image Quant software (on an Intel 80486 microprocessor). GC-MS analysis of derivatized samples was performed using a Hewlett-Packard 5890 Gas Chromatograph and a Micromass Trio2000 Quadrupole Mass Spectrometer. GC-MS was conducted using a DB-5 column, a source temperature of 200 °C and an oven temperature gradient as follows: 140 °C for 1 min, increase at 25 °C /min to 215 °C, increase at 6 °C /min to 240 °C, increase at 70 °C /min to 280 °C, hold at 280 °C for three

min. Autosampling of 2 μL injections was performed using a Hewlett-Packard 7674a Autosampler and data analysis was performed using Windows based Micromass MassLynx software. Electrospray ionization-mass spectrometry (ESMS) was performed using a Kratos Analytical Ltd. Profile Mass Spectrometer and Mach 3 software.

HPLC was performed on an SSI 200B/220B dual pump system with an SSI controller and a Rainin UV-D II detector (output to a Linear 255/M recorder and an HP 3390A electronic integrator). Solvent gradients were run at 10 mL/min for preparative separations (Rainin, 300 Å, C_{18}, 250 mm x 21.4 mm column) and either 1 mL/min or 2 mL/min for analytical separations (Alltech, 5-μm, C_{18}, 250 mm x 4.6 mm Econosphere column). Gradient A: solvent A, 10 mM triethyl ammonium acetate (pH 7.0); solvent B, 50% 10 mM triethyl ammonium acetate and 50% acetonitrile; a 10-min linear gradient from 60% A to 40% A, isocratic 40% A for 15 min, and a 5-min linear gradient to initial conditions. Gradient B: solvent A, 50 mM ammonium acetate (pH 4.0); solvent B, acetonitrile; isocratic 50% A. Gradient C: solvent A, 100 mM ammonium acetate (pH 7.0); solvent B, acetonitrile; initial 3-min isocratic t 9% B, a 20-min linear gradient from 9% B to 18% B, a 5-min isocratic at 18% B, and a 5-min linear gradient return to initial conditions of 9% B. Gradient D: solvent A, 10 mM ammonium acetate (pH 7.0); solvent B, acetonitrile; initial 7-min isocratic at 8% B, a 10-min linear gradient from 8% B to 30% B, a 5-min isocratic at 30% B, and a 5-min linear gradient return to initial conditions of 8% B.

Synthesis and Purification of Oligodeoxynucleotides. Each of the oligodeoxynucleotides used in this dissertation were synthesized using standard phosphoramidite methodology without removing the dimethoxytrityl group on the 5'

end. Oligodeoxynucleotides were synthesized in either 10 μmol or 1 μmol quantities After 12-14 hours of deprotection with concentrated ammonium hydroxide at 55 °C, the sample was concentrated and purified by preparative scale HPLC using gradient A. After concentration of the purified DNA, the DNA was detritylated by treatment with 10% acetic acid for 1 hour. In order to ethanol precipitate the DNA, 3 M sodium acetate (pH 5.2) was added to bring the aqueous solution to a concentration of 0.3 M and cold ethanol was added (-20°C) such that the final volumetric ratio of EtOH:H_2O was 85:15. This was kept at -20 °C for 1 hour and centrifuged for 15 minutes at 4 °C. The supernatant was removed and resulting pellet was dried using a speed-vac.

Preparation of Radiolabeled DNA. Oligonucleotides were 5'-radiolabeled using the following procedure: 0.01 - 0.1 O.D. of DNA was placed in a microfuge tube and diluted to 14 μL with water. Added to this was 2 μL of 10x kinase buffer [0.5 M Tris (pH 7.5), 0.1 M $MgCl_2$, 50 mM DTT, 1 mM spermidine, 1 mM EDTA], 1 μL (10 μCi) of [γ-^{32}P] ATP, and 1 μL (3 units) of T4 polynucleotide kinase. This was incubated at 37 °C for 30 minutes. Radiolabeling was stopped by heating the reactions at 90 °C for 5 minutes followed by ethanol precipitation.

Reactions of DNA duplex I with Adriamycin in the Presence of Either CH_2O, DTT/Fe^{3+}, or H_2O_2. 5'-radiolabeled 5'-d(TTG AAG CAA CGA AGT T) was annealed to 5'-d(AAC TTC GTT GCT TCA A) by heating to 90°C for 5 minutes and cooling to room temperature over approximately 1 hour. Reaction mixtures were comprised of duplex DNA (100 μM) and adriamycin (200 μM, $\varepsilon_{(480)}$ = 11,500) in buffered solution (40 mM Tris base, pH 8.0, 50 mM KCl, 3 mM $MgCl_2$, 0.1 mM EDTA) and were incubated in the dark at 37 °C. In order that both DPAGE and GC-MS analysis could be performed, 2 - 20 μL aliquots were taken in each case and

quenched by ethanol precipitation. CH_2O: reaction mixtures (40 μL volume, giving 2 - 20 μL aliquots) were incubated with varying concentrations of CH_2O and allowed to progress for 24 hours. DTT/Fe^{3+}: reactions were identical except for the absence of CH_2O and the addition of 7 mM dithiothreitol and 40 μM $Fe(Cl)_3$. H_2O_2: reaction mixtures were identical except for the absence of CH_2O and the addition of 5 mM H_2O_2. Reactions with either DTT/Fe^{3+} or H_2O_2 were allowed to proceed for 96 hours and were done in triplicate (200 μL initial volume, giving 2 - 20 μL aliquots at each of 5 time points (0, 24, 48, 72, and 96 h)).

Aliquots of 20 μL from reactions that had been ethanol precipitated were dissolved in gel loading buffer (5 M urea, 0.5% xylene cyanol) and analyzed by DPAGE. DPAGE was conducted on a 20% gel (19:1 acrylamide:bisacryalmide) with 8 M urea in 1 X TBE buffer (0.35 mm thick, 33cm x 41 cm, using either 20- or 40-toothed comb). Gels were run at 2000 V with the refrigerated circulator kept at 15°C. They were run until the xylene cyanol dye had run 10 cm (approximately 3 hours). The gel was transferred to Saran Wrap and filter paper, dried for 40 minutes at 80°C, and visualized by either autoradiography or phosphorimagery.

Synthesis of N-methyl adriamycin (1b). The reaction mixture was assembled in no particular order and comprised of adriamycin (100 μM), $NaCNBH_3$ (67 μM), and CH_2O (2.5 mM) in 2:1 CH_3CN:H_2O. After 1.5 h at room temperature, the reaction mixture was analyzed by analytical HPLC using gradient B. This gave three broad peaks, the first of which was determined by comparison of retention times and co-injection to be adriamycin. The second and third peaks were determined by ESMS to be N-methyl adriamycin (**1b**) (MH^+ = 558.5) and N,N-dimethyl adriamycin (**1c**) (MH^+ = 572.5), respectively. Subsequent GC-MS analysis of adriamycin and **1b** after

borohydride reduction and acetylation showed three major ions for each (**14a**: m/e 56, 98, 158; **14b**: m/e 70, 112, 172). This is consistent with methylation having occurred at the amino group.

GC-MS Analyses. 10 μL solutions of either adriamycin, N-methyl adriamycin (**1b**), or a 1:1 mixture of both were subjected to GC-MS analysis. The procedure that follows is similar to methodology by Blakeney *et al.(64)* First, 5 μL of 10 mM glucosamine was added as an internal standard. 50 μL aqueous 5 M $NaBH_4$ was added, the microfuge used as the reaction vessel was pierced with a needle in order to prevent pressure from building up, and the reduction allowed to progress at 65°C for 1.5 h. 50 μL of glacial acetic acid was added to consume the excess $NaBH_4$. 100 μL N-methyl imidazole and 1 mL acetic anhydride were added to acetylate the amino sugars. After 30 minutes at room temperature, the acetic anhydride was quenched by addition of 2 mL H_2O and the acetylated amino sugars extracted with 1 mL CH_2Cl_2. The extracted CH_2Cl_2 was removed by speed-vac and the sample dissolved in 100 μL CH_3CN and subjected to GC-MS analysis. After monitoring the total ion current (TIC) of the GC-MS, the retention times of **14a**, **14b**, and the internal standard were determined. After this, single-ion monitoring (SIM) was used to more precisely measure the most intense signals for **14a** (98.1), **14b** (112.1), and the internal glucosamine standard (84.1).

Known concentrations of **1b** (determined by UV/Vis assuming that **1b** and adriamycin have the same extinction coefficient) were mixed with the internal standard glucosamine and subjected to borohydride reduction, acetylation, and GC-MS analysis. The ratios of the size of these peaks were then used to determine the concentration of **14b** detected in the subsequent experiments. Treatment of samples from the DTT/Fe^{3+},

H_2O_2, and CH_2O activated reactions was the same as above, except that an ethanol-precipitated DNA pellet was the original sample.

Preparative Scale Reactions of DNA with Adriamycin and Either DTT/Fe^{3+} or H_2O_2. Non-radiolabeled DNA duplex I was reacted with either DTT/Fe^{3+} or H_2O_2 at the same concentrations as the analytical reactions (1 mL volume). After ethanol precipitation, the DNA was dissolved in gel loading buffer and purified on 20% DPAGE (1.5 mm thick, 14 x 16 cm, using a five-toothed comb). The gel was run at 350 V at room temperature until the xylene cyanol dye had run 4 cm (approximately 2 h). The single stranded (SS) and double stranded (DS) DNA bands for each activating agent were located by UV shadowing and isolated from the gel by a crush and soak procedure: gel slices were crushed with a glass rod into fine particles and incubated at 4 °C for 30 minutes with elution buffer (500 mM ammonium acetate (pH 7.0), 10 mM $MgCl_2$, and 10 mM Na_2EDTA). The cold temperature and short duration of the elution procedure was required to minimize decomposition of lesion **2**. The solution containing DNA was separated from gel particles by centrifugation and the DNA was desalted using a Waters Sep-Pak C_{18} cartridge: a Sep-Pak was attached to a plastic syringe (10 mL size) and washed with 10 mL of CH_3CN followed by 10 mL of H_2O. The aqueous solution containing DNA sample was then loaded to the cartridge through the syringe. The Sep-Pak was sequentially washed with 10 mL of 10 mM ammonium acetate and 10 mL H_2O; and the DNA eluted with 4 mL 25% aqueous CH_3CN which was subsequently frozen and concentrated to dryness.

Pelleted DNA isolated from SS and DS DNA were each brought up in 40 μL H_2O and split into 2 - 20 μL aliquots. For each sample, the internal standard glucosamine and $NaBH_4$ were added to one aliquot, with the subsequent derivatization

and GC-MS analysis. The other 20 μL aliquot had 4 μL alkaline phosphatase (4 units) and 1 _L phosphodiesterase I (1 unit) added and incubated at 37°C in the dark overnight in order to enzymatically digest the DNA. The concentration of digested DNA duplex I ($\varepsilon_{(260)}$=360,000) and adriamycin ($\varepsilon_{(480)}$ = 11,500) in the original 20 μL aliquots were then determined by bringing the volume of the solutions to 1 mL and measuring the UV/Vis spectrum.

Reactions of DNA duplex II, III, IV, and V with Adriamycin in the Presence of Various Amounts of CH_2O. Duplexes were assembled by annealing equivalent amounts of the two single strands in the same method used for duplex I. The DNA duplexes (50 μM) were then incubated (40 mM Tris base, pH 8.0, 50 mM KCl, 3 mM $MgCl_2$, 0.1 mM EDTA) in the dark at 37°C with adriamycin (50 μM) with various concentrations of formaldehyde for 24 hours (0-5000 μM). These samples were then ethanol precipitated, reduced by borohydride, acetylated, and analyzed by GC-MS similar to the previously outlined methods.

Platination of small amounts of DNA (less than 10 O.D. units). 3 mg of cis-diaminedichloroplatinum(II) (M.W. 300.06) was stirred in 1 mL water in an eppendorf tube overnight in the dark in order to activate the cisplatin (generating a 10 mM solution). Activation involves replacement of the chloride ions with water molecules. Approximately 3.0 O.D. units of the single standed DNA 15-mer were combined with 7.5 μL of this 10 mM solution and water added to bring the total volume to 250 μL. The resulting concentrations of the DNA and activated platinum complex are 100 μM and 300 μM, respectively. This mixture is allowed to react in the dark at 37°C and followed by analytical HPLC using gradient C. Once the reaction appears to have gone to at least 50% completion (judged by the appearance of longer retention time

peaks on HPLC), usually after approximately 2 hours, the various peaks are purified using HPLC. The normal retention time for the native 15-mers was approximately 15 minutes, with the cisplatin intrastrand crosslink having a retention time approximately 1-2 minutes later. Fractions were isolated and dried down in the SpeedVac concentrator. Isolated fractions were determined to be the cisplatin intrastrand crosslink by HPLC analysis.

Platination of sequence D to generate NMR-sized sample. 10 mg of cis-diaminedichloroplatinum(II) (M.W. 300.06) was dissolved in 400 μL of water and stirred in the dark overnight. Approximately 200 O.D. units of single-stranded D in 1 mL of water had 100 μL of this cisplatin solution added to it and was allowed to react in the dark at 37°C. The progress of the reaction was followed by analytical HPLC using gradient C until a sufficient amount of cross-linked DNA was formed (approximately 4 hours). At this stage, the various peaks were collected using preparative-scale HPLC and gradient C. The peaks were dried down by SpeedVac concentration and the presence of the crosslink was determined by HPLC analysis of enzymatic digestion and negative-ion electrospray mass spectrometry.

Enzymatic digestion and HPLC analysis of platinated DNA. Between 0.1 and 1.0 O.D. units of DNA are combined with 1 μL of snake venom phosphodiesterase I (1 unit), 2 μL of calf alkaline phosphatase (2 units), 2 μL of 10 x alkaline phospatase buffer, and brought to a final volume of 20 μL. This is then allowed to digest at 37°C in the dark for at least 1 hour. This is then analyzed by analytical HPLC using gradient D. The approximate retention times of each of the nucleosides are: deoxycytosine, 3 min.; deoxyguanosine, 5 min.; deoxythymidine, 6 min.; deoxyadenosine, 9 min. These retention times can vary according to the age of the column used. The order of their

appearance, however, does not change. Cisplatin intrastrand crosslinks were indicated by the absence of deoxyguanosine (dG) from the HPLC chromatagram. This is due to the fact that the single-stranded oligonucleotides used only had two dG's, centrally and adjacently located, in their sequence.

Negative-ion ESMS of oligonucleotides. Electrospray mass spectrometry in the negative ion mode was performed on a VG quattroII/MassLynx PC DS triple quadrupole mass spectrometer [4000 Da (Q1+Q3), unit resolution (Q1 +Q3)] at the Medicinal Chemistry Mass Spectrometry facility, University of Washington. Samples were infused at a flow rate of 0.01 mL/min with a mobile phase of 80% MeOH and 0.05% NH_4OH ion H_2O, 100° C, probe voltage 3.4 KV, HV lens 0.9 KV, cone 30 V. Data acquistion was 200-2000 Da in 42 seconds. Data was processed by the Maximum Entropy (MaxEnt) algorithm at 5.0 or smaller resolution.

Negative-ion ESMS followed by MaxEnt analysis showed calculated masses corresponding to the predicted molecular weights for each of the native single-stranded oligonucleotides. The predicted molecular weight of any of these corresponds to the mass of the neutral species. In the case of a single-stranded DNA, this corresponds to the molecular weight using H^+ as a counter-ion for each phosphate. For example, in the case of a 15-mer, one would add 14 a.m.u. to the molecular weight of the entire DNA strand to account for the 14 inter-joining phosphates. With the addition of the cisplatin intrastrand crosslink, the molecular weight increased by 229 a.m.u., but the platinum (II) removes two charge equivalents from the overall oligonucleotides. As a result the MaxEnt analysis shows an increase in the molecular weight of the neutral species of approximately 227 a.m.u. The resolution of MaxEnt analysis is ± 5 a.m.u., and the cisplatin intrastrand crosslinks consistently had calculated masses well within this range.

Direct binding with xUBF Box 1. Relevant duplexes and 4-way junction DNA's were assembled by combining respective components of these DNA probes in a 1:1 ratio. One of these strands was 5'-radiolabeled in order to visualize the location of the DNA probe on the gel. These probes were assembled in the appropriate buffer of the experiment. In order to anneal, these DNA's were heated to a temperature of 90°C for five minutes on a heating block and then allowed to cool to room temperature by turning the heating block off. It took approximately 1 hour for this cooling and annealing process to finish. The DNA probe was then mixed with increasing concentrations of xUBF Box 1 in a total volume of 20-40 μL and allowed to incubate in an ice bath for at least 20 minutes. After this, 50% aqueous glycerol was added to make the toal concentration of glycerol 12.5%. This was done to increase the density of the samples for easier loading on gel electrophoresis equipment.

Competition binding with 4-way junction DNA and xUBF Box 1. 4-way junction DNA was assembled by annealing 5'-radiolabeled 1sTT2s strand with 1.1 equivalents of 3sTT4s strand (sequences in Fig. 26, p. 56). This 4-way junction DNA was then mixed with a specific concentration of xUBF Box 1 in buffer previously used by Lippard (10 mM HEPES, 10 mM $MgCl_2$, 100 mM NaCl, 1 mM spermidine, 2 mg/mL bovine serum albumin, 0.05% Nonidet P-40, pH 7.5).(*87*) The concentration of xUBF Box 1 was either 100 nm or 200 nm. After 20 minutes on ice, 20 μL aliquots of this bulk solution was mixed with several different 20 μL samples containing increasing concentrations of competitor DNA probe. This competitor DNA probe was in the same buffer conditions. This 3-component binding mixture was then also incubated on ice for 20 minutes. After this, 50% aqueous glycerol was added to bring the concentration of glycerol to 12.5 % and the samples were analyzed by native PAGE.

Native polyacrylamide gel electrophoresis (PAGE) analysis of xUBF binding. Samples from either direct binding or 4-way junction competition experiments were run on 10% Native Gels (29:1 acrylamide:bisacrylamide, 0.5 x TBE buffer, 10% in glycerol, 0.75 mm gel, Hoeffer submersible gel stand). The native gel was run (200 V, 0.5 X in TBE, in a 4°C cold room, 2 – 2 1/2 hours). The gel was then dried using the gel dryer (80°C, 30 min.) and then phosphorimaged (1-16 hours). Phosphorimagery analysis was then performed using Molecular Dynamics' ImageQuant software (v. 4.2a) to determine the relative size of bands.

Determination of K_d's between DNA probes and xUBF Box 1. Curve-fitting was performed with MacCurveFit software (v.1.3.3) in the Quasi-Newton Method. For determination of the K_d of the 4-way junction with xUBF Box 1, the fraction of 4-way junction free was plotted vs. the concentration of xUBF Box 1. Curve-fitting was then performed for $y = K_d/(K_d + x)$ and the value of K_d determined. In the case of the competition assay, the fraction of 4-way junction bound to protein was plotted vs. the concentration of competitor DNA (concentration of xUBF Box 1 is kept constant). Curve-fitting was then performed for:

$$y_x = \frac{y_0 * K_{d_{DNA}}}{x * (1-y_0) + K_{d_{DNA}}}$$

y_0 = 4wj bound (original)

y_x = 4wj bound

x = [comp. DNA]

In this manner, the K_d of the probe DNA was determined.

References:

1. Franks, L. M., and Teich, N. M. (1986) *Introduction to the cellular and molecular biology of cancer*, Oxford University Press, Oxford [Oxfordshire] ; New York.
2. Pratt, W. B., Ruddon, R. W., Ensminger, W. D., and Maybaum, J. (1994) *The Anticancer Drugs*, 2nd ed., Oxford University Press, Inc., New York.
3. Macdonald, F., and Ford, C. H. J. (1997) *Molecular Biology of Cancer*, BIOS Scientific Publishers Ltd., Oxford.
4. Sarma, R. H., and Sarma, M. H. (1988) *DNA double helix & the chemistry of cancer*, Adenine Press, Schenectady, N.Y.
5. American Cancer Society (1994) *Cancer Facts & Figures*, American Cancer Society, Atlanta, GA.
6. Frezard, F., and Garnier-Suillerot, A. (1991) *Biochemistry 30*, 5038-43.
7. Gigli, M., Doglia, S. M., Millot, J. M., Valentini, L., and Manfait, M. (1988) *Biochim Biophys Acta 950*, 13-20.
8. Schwartz, H. S. (1983) in *Molecular Aspects of Anticancer Drug Design* (Neidle, S., and Waring, M. J., Eds.) pp 93-126, MacMillan Press, London.
9. Valentini, L., Nicolella, V., Vannini, E., Menozzi, M., Penco, S., and Arcamone, F. (1985) *Farmaco [Sci] 40*, 377-90.
10. Cummings, J., and McArdle, C. S. (1986) *Br J Cancer 53*, 835-8.
11. Watson, J. W., and Crick, F. H. C. (1953) *Nature 171*, 737.
12. Bishop, J. M., Weinberg, R. A., and Scientific American Inc. (1996) *Scientific American molecular oncology*, Scientific American, New York.
13. Ruddon, R. W. (1995) *Cancer biology*, 3rd ed., Oxford University Press, New York.
14. Ross, D. W. (1998) *Introduction to Oncogenes and Moelecular Cancer Medicine*, Springer-Verlag, Inc., New York.

15. Doroshow, J. H. (1996) in *Cancer Chemotherapy and Biotherapy: Principles and Practice* (Chabner, B. A., and Longo, D. L., Eds.) pp 409-434, Lippincott-Raven, Philadelphia.

16. Despois, R., Dubost, M., Mancy, D., Maral, R., Ninet, L., Pinnert, J., Preud'Homme, J., Charpentie, Y., Belloc, A., de Chezelles, N., Lunel, J., and Renaut, J. (1967) *Arznein.-Forsch. 17*, 934.

17. Dubost, M., Ganter, P., Maral, R., Ninet, L., Pinnert, S., Preud'Homme, J., and Werner, G. H. (1963) *C. R. Acad. Sci. 257*, 1813.

18. Grein, A., Spalla, C., Di Marco, A., and Canevazzi, G. (1963) *G. Microbiol. 11*, 109.

19. Cassinelli, G., and Orezzi, P. (1963) *G. Microbiol. 11*, 109.

20. Weiss, R. B. (1992) *Semin Oncol 19*, 670-86.

21. Di Marco, A., Gaetani, M., Dorigotti, l., Soldati, M., and Bellini, O. (1963) *Tumori 49*, 235.

22. Bernard, J., Paul, R., Boiron, M., Jacquillat, C., and Maral, R. (1969) *Recent Results Cancer Res. 20*, 1.

23. Arcamone, F., Franceschi, G., Orezzi, P., Cassinelli, G., Barbieri, W., and Mondelli, R. (1964) *J. Am. Chem. Soc. 86*, 5334.

24. Arcamone, F., Cassinelli, G., Orezzi, P., Franceschi, G., and Mondelli, R. (1964) *J. Am. Chem. Soc. 86*, 5335.

25. Di Marco, A., Gaetani, M., and Scarpinato, B. (1969) *Cancer Chemother Rep 53*, 33-7.

26. Jones, S. E. (1982) *Current Concepts in the Use of Doxorubicin Chemotherapy*, Farmitalia Carlo Erba, Milano.

27. De Vita, V. T., Hellman, S., and Rosenberg, S. A. (1989) *Cancer: Principles and Practice of Oncology*, 34th ed., Lippincot, Philadelphia.

28. Chabner, B., and Collins, J. M. (1990) *Cancer chemotherapy : principles and practice*, Lippincott, Philadelphia.

29. Chabner, B., and Longo, D. (1996) *Cancer Chemotherapy and Biotherapy*, Lippincott-Raven, Philadelphia.

30. Gilladoga, A. C., Manuel, C., Tan, C. T., Wollner, N., Sternberg, S. S., and Murphy, M. L. (1976) *Cancer 37*, 1070-8.

31. Lenaz, L., and Page, J. A. (1976) *Cancer Treat Rev 3*, 111-20.

32. Singal, P. K., Iliskovic, N., Li, T., and Kumar, D. (1997) *Faseb J 11*, 931-6.

33. Gewirtz, D. A. (1999) *Biochem Pharmacol 57*, 727-41.

34. Chaires, J. B., Satyanarayana, S., Suh, D., Fokt, I., Przewioka, T., and Priebe, W. (1996) *Biochemistry 35*, 2047-53.

35. Koch, T. H., and Gaudiano, G. (1995) in *Anthracycline Antibiotics* (Priebe, W., Ed.) pp 115-131, American Chemical Society, Washington, DC.

36. Bachur, N. R., Jonson, R., Yu, F., Hickey, R., and Malkas, L. (1995) in *Anthracycline Antibiotics* (Priebe, W., Ed.) pp 204-221, American Chemical Society, Washington, DC.

37. Tuteja, N., Phan, T. N., Tuteja, R., Ochem, A., and Falaschi, A. (1997) *Biochem Biophys Res Commun 236*, 636-40.

38. Bachur, N. R., Lun, L., Sun, P. M., Trubey, C. M., Elliott, E. E., Egorin, M. J., Malkas, L., and Hickey, R. (1998) *Biochem Pharmacol 55*, 1025-34.

39. Bachur, N. R., Johnson, R., Yu, F., Hickey, R., Applegren, N., and Malkas, L. (1993) *Mol Pharmacol 44*, 1064-9.

40. Liu, L. F. (1989) *Annu Rev Biochem 58*, 351-75.

41. Capranico, G., and Zunino, F. (1992) *Eur J Cancer 12*, 2055-60.

42. Potmesil, M. (1988) in *Anthracycline and Anthracenedione-Based Anticancer Agents* (Lown, J. W., Ed.) pp 447-474, Elsevier, Amsterdam.

43. Pommier, Y. (1995) in *Anthracycline Antibiotics* (Priebe, W., Ed.) pp 183-203, American Chemical Society, Washington, DC.

44. Frederick, C. A., Williams, L. D., Ughetto, G., van der Marel, G. A., van Boom, J. H., Rich, A., and Wang, A. H. (1990) *Biochemistry 29*, 2538-49.

45. Wang, A. H., Ughetto, G., Quigley, G. J., and Rich, A. (1987) *Biochemistry 26*, 1152-63.

46. Wang, A. H., Gao, Y. G., Liaw, Y. C., and Li, Y. K. (1991) *Biochemistry 30*, 3812-5.

47. Wang, J., Chao, M., and Wang, A. H. (1995) in *Anthracycline Antibiotics* (Priebe, W., Ed.) pp 168-182, American Chemical Society, Washington, DC.

48. Cullinane, C., van Rosmalen, A., and Phillips, D. R. (1994) *Biochemistry 33*, 4632-8.

49. Cutts, S. M., and Phillips, D. R. (1995) *Nucleic Acids Res 23*, 2450-6.

50. Cullinane, C., and Phillips, D. R. (1990) *Biochemistry 29*, 5638-46.

51. Cullinane, C., Cutts, S. M., van Rosmalen, A., and Phillips, D. R. (1994) *Nucleic Acids Res 22*, 2296-303.

52. Egholm, M., and Koch , T. H. (1989) *Journal of the American Chemical Society 111*, 8291-8293.

53. Taatjes, D. J., Gaudiano, G., Resing, K., and Koch, T. H. (1996) *J Med Chem 39*, 4135-8.

54. Taatjes, D. J., Gaudiano, G., Resing, K., and Koch, T. H. (1997) *J Med Chem 40*, 1276-86.

55. Taatjes, D. J., Gaudiano, G., and Koch, T. H. (1997) *Chem Res Toxicol 10*, 953-61.

56. Leng, F., Savkur, R., Fokt, I., Przewioka, T., Priebe, W., and Chaires, J. B. (1996) *Journal of American Chemical Society 118*, 731-738.

57. Zeman, S. M., Phillips, D. R., and Crothers, D. M. (1998) *Proc Natl Acad Sci U S A 95*, 11561-5.

58. van Rosmalen, A., Cullinane, C., Cutts, S. M., and Phillips, D. R. (1995) *Nucleic Acids Res 23*, 42-50.

59. Katritzky, A. R., Yannakopoulou, K., and Lang, H. (1994) *J. Chem. Soc Perkin Transactions 2 8*, 1867-1870.

60. Bîhme, H., and Eichler, D. (1967) *Chem. Ber. 100*, 2131-2137.

61. Huang, H., and Hopkins, P. B. (1993) *J Am Chem Soc 115*, 1199.

62. Cherif, A., and Farquhar, D. (1992) *J Med Chem 35*, 3208-14.

63. Henry, R. J., Blakeney, A. B., Harris, P. J., and Stone, B. A. (1983) *J Chromatogr 256*, 419-27.

64. Blakeney, A. B., Harris, P. J., Henry, R. J., and Stone, B. A. (1983) *Carbohydrate Research 113*, 291.

65. Chaires, J. B. (1983) *Biochemistry 22*, 4204-11.

66. Chaires, J. B., Herrera, J. E., and Waring, M. J. (1990) *Biochemistry 29*, 6145-53.

67. Acton, E. M., Tong, G. L., Mosher, C. W., and Wolgemuth, R. L. (1984) *J Med Chem 27*, 638-45.

68. Nagy, A., Armatis, P., and Schally, A. V. (1996) *Proc Natl Acad Sci U S A 93*, 2464-9.

69. Zwelling, L. A., Altschuler, E., Cherif, A., and Farquhar, D. (1991) *Cancer Res 51*, 6704-7.

70. Feniuc, D., Taatjes, D., and Koch, T. (1997) *Journal of Medicinal Chemistry 40*, 2452-2461.

71. Jantzen, H. M., Admon, A., Bell, S. P., and Tjian, R. (1990) *Nature 344*, 830-6.

72. Laudet, V., Stehelin, D., and Clevers, H. (1993) *Nucleic Acids Res 21*, 2493-501.

72b. Weir, H. M., Kraulis, P. J., Hill, C. S., Raine, A. R., Laue, E. D., and Thomas, J. O. (1993) *Embo J 12*, 1311-9.

73. Bianchi, M. E., Beltrame, M., and Paonessa, G. (1989) *Science 243*, 1056-9.

74. Pil, P. M., and Lippard, S. J. (1992) *Science 256*, 234-7.

75. Fischhaber, P. (1998) in *Chemistry* pp 127, University of Washington, Seattle.

76. Hu, C. H., McStay, B., Jeong, S. W., and Reeder, R. H. (1994) *Mol Cell Biol 14*, 2871-82.

77. Rosenberg, B., Van Camp, L., and Krigas, T. (1965) *Nature 205*, 698.

78. Rosenberg, B., VanCamp, L., Trosko, J. E., and Mansour, V. H. (1969) *Nature 222*, 385-6.

79. Eastman, A. (1986) *Biochemistry 25*, 3912-5.

80. Eastman, A. (1987) *Pharmacol Ther 34*, 155-66.

81. Fichtinger-Schepman, A. M., van der Veer, J. L., den Hartog, J. H., Lohman, P. H., and Reedijk, J. (1985) *Biochemistry 24*, 707-13.

82. Reed, E., Ozols, R. F., Tarone, R., Yuspa, S. H., and Poirier, M. C. (1987) *Proc Natl Acad Sci U S A 84*, 5024-8.

83. Trimmer, E. E., Zamble, D. B., Lippard, S. J., and Essigmann, J. M. (1998) *Biochemistry 37*, 352-62.

84. Ohndorf, U. M., Whitehead, J. P., Raju, N. L., and Lippard, S. J. (1997) *Biochemistry 36*, 14807-15.

85. Whitehead, J. P., and Lippard, S. J. (1996) *Met Ions Biol Syst 32*, 687-726.

86. Chow, C. S., Barnes, C. M., and Lippard, S. J. (1995) *Biochemistry 34*, 2956-64.

87. Dunham, S. U., and Lippard, S. J. (1997) *Biochemistry 36*, 11428-36.

88. Fischhaber, P. (1998) .

89. Putnam, C. D., and Pikaard, C. S. (1992) *Mol Cell Biol 12*, 4970-80.

90. Harwood, E. A. (1999) in *Chemistry*, University of Washington, Seattle.

91. Treiber, D. K., Zhai, X., Jantzen, H. M., and Essigmann, J. M. (1994) *Proc Natl Acad Sci U S A 91*, 5672-6.

92. Zhai, X., Beckmann, H., Jantzen, H. M., and Essigmann, J. M. (1998) *Biochemistry 37*, 16307-15.

93. Chao, J. C., Wan, X. S., Engelsberg, B. N., Rothblum, L. I., and Billings, P. C. (1996) *Biochim Biophys Acta 1307*, 213-9.

94. Codony-Servat, J., Gimeno, R., Gelpi, C., Rodriguez-Sanchez, J. L., and Juarez, C. (1996) *Biochem Pharmacol 51*, 1131-6.

Vita

Ryan Austin Luce was born in Pittsburgh, Pennsylvania on July 12, 1972. He was raised largely in Lee's Summit, Missouri. He majored in chemistry at Duke University where he received his Bachelor of Science degree in 1994. He began graduate work in the fall of 1994 at the University of Washington in Seattle and received his Ph.D. in 1999.